Regulating *prospero* mRNA stability determines when neural stem cells stop dividing

Authors Lu Yang[1], Tamsin J. Samuels[1], Yoav Arava[1,2], Francesca Robertson[1], Aino I. Järvelin[1], Ching-Po Yang[3], Tzumin Lee[3], David Ish-Horowicz[1,4] and Ilan Davis[1*]

Affiliations

[1]Department of Biochemistry, The University of Oxford, UK.
[2]Technion, Haifa, Israel.
[3]Janelia Research Campus, Virginia, USA.
[4]MRC Laboratory for Molecular Cell Biology, University College, London, UK.

Graphical Abstract

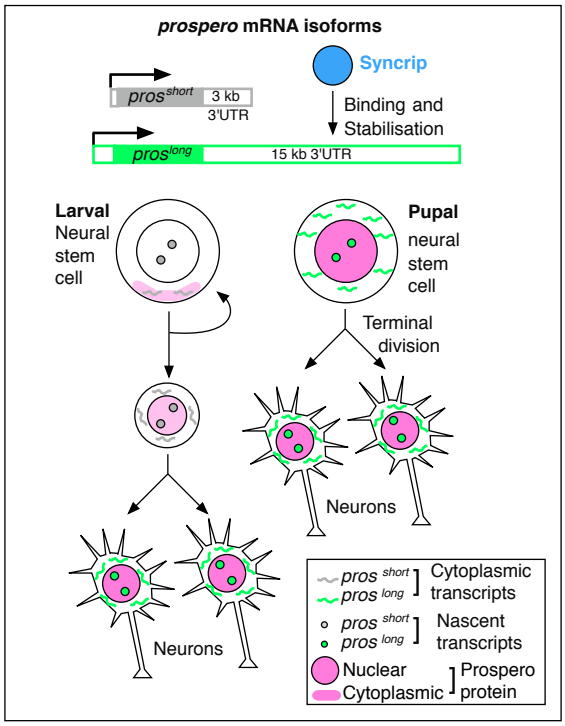

Correspondence

ilan.davis@bioch.ox.ac.uk Phone: +44 (0) 1865 613265

In brief

We have discovered that a novel mechanism of regulated mRNA stability produces an expression peak of Prospero, the conserved transcriptional regulator that stops neural stem cells dividing during brain development. Syncrip, a conserved mRNA-binding protein, stabilises a cell-type-specific isoform of *prospero* mRNA containing an unusually long 3' UTR.

Highlights

- Single molecule FISH shows that *prospero* levels are post-transcriptionally regulated
- Syncrip binds and stabilises a long isoform of *prospero* mRNA with a 15 kb 3' UTR
- Long *prospero* is transcribed and stabilised in terminally dividing neural stem cells
- Syncrip and long *prospero* are required to terminate neural stem cell divisions

Keywords *Drosophila*, larvae, pupae, central nervous system, neural stem cells, neuroblasts, mRNA stability, post-transcriptional regulation, gene expression, transcription factors, homeobox, single molecule FISH, Prospero, Prox1, Syncrip, hnRNPQ, 3' UTR, mRNA-binding proteins.

Regulating *prospero* mRNA stability determines when neural stem cells stop dividing

Lu Yang[1], Tamsin J. Samuels[1], Yoav Arava[1,2], Francesca Robertson[1], Aino I. Järvelin[1], Ching-Po Yang[3], Tzumin Lee[3], David Ish-Horowicz[1,4] and Ilan Davis[1*]
[1]Department of Biochemistry, The University of Oxford, UK.
[2]Technion, Haifa, Israel.
[3]Janelia Research Campus, Virginia, USA.
[4]MRC Laboratory for Molecular Cell Biology, University College, London, UK.

*Correspondence: ilan.davis@bioch.ox.ac.uk

SUMMARY

During *Drosophila* and vertebrate brain development, termination of neural stem cell (neuroblast) proliferation and their differentiation require the conserved transcription factor Prospero/Prox1. It is not known how the level of Prospero is regulated to produce an expression peak in pupal neuroblasts, which terminates proliferation. Here, we use single molecule fluorescent *in situ* hybridisation to show that larval neurons and terminal pupal neuroblasts selectively transcribe a long *prospero* isoform containing a 15 kb 3' UTR stabilised by binding to the conserved RNA-binding protein Syncrip/hnRNPQ. The long *prospero* isoform and Syncrip are both required to stop neuroblasts dividing. Our results demonstrate an unexpected function for mRNA stability in limiting neuroblast proliferation required for normal brain development. Given that Prox1 regulates vertebrate neuroblasts and other stem cells, our findings suggest widespread roles for regulated mRNA stability in stem cell biology.

INTRODUCTION

The central nervous system (CNS) consists of a huge diversity and number of neurons and glia that originate from a limited population of neural stem cells, also known as neuroblasts (NBs) (Kelava and Lancaster, 2016). To produce a normal CNS, NBs must divide the correct number of times and undergo a precisely regulated programme of differentiation. Many factors and mechanisms regulating these processes have been studied in great detail, and in many cases are conserved between vertebrates and *Drosophila* (Homem and Knoblich, 2012). However, a key question in both vertebrates and *Drosophila* CNS development is how NB numbers are regulated by balancing proliferation and differentiation; this question has not yet been conclusively answered.

In *Drosophila* embryos and larvae, NBs divide asymmetrically, multiple times, while maintaining a single large cell that retains its stem cell properties. The asymmetric NB divisions 'bud off'

smaller cells, called ganglion mother cells (GMCs) (Knoblich, 2008) that typically divide only once to produce a pair of differentiated cells (Homem and Knoblich, 2012). There are two classes of NB lineages; type I, in which GMCs originate directly form the NB divisions, and type II, in which NBs divide to give intermediate neuronal progenitors (INPs) that are stem cell-like in character, and divide further to generate multiple GMCs (Homem and Knoblich, 2012). Type I proliferation and differentiation are determined by the conserved homeodomain containing transcriptional regulator, Prospero (Pros) (Bayraktar et al., 2010). Pros activates the expression of genes required for the differentiation of type I NB progeny and suppresses the expression of genes required to promote stem-like properties (Lai and Doe 2014; Doe *et al.,* 1991; Vaessin *et al.,* 1991; Matsuzaki *et al.,* 1992; Choksi *et al.,* 2006; Bello *et al.,* 2006; Betschinger *et al.,* 2006; Lee *et al.,* 2006). In contrast, type II NBs do not express Pros and their progeny remain stem cell-like as they have no immediate need for balancing proliferation and differentiation (Bayraktar et al., 2010). Prox1, the highly conserved vertebrate homologue of Pros, has related roles in the regulation of stem cells in diverse tissues (Kato *et al.,* 2015; Dyer *et al.,* 2002; Foskolou *et al.,* 2013; Stergiopoulous *et al.,* 2015; Elsir *et al.,* 2012), but less is known about the details of Prox1 expression and function in comparison to Pros.

The best understood function of Pros is in promoting the differentiation of the progeny of NB into GMCs and then further into neurons. *pros* mRNA and Pros protein are segregated asymmetrically during NB division (Hirata *et al.,* 1995; Spana and Doe, 1995; Knoblich *et al.,* 1995), a process most extensively studied in embryos, but also operating in larvae (Kitajima *et al.,* 2010). Pros is first expressed in NBs and is localised in a cortical basal crescent through binding to Miranda (Mir) protein, which prevents the import of Pros into the NB nucleus and ensures its inheritance by the GMC. Once Mir is degraded, Pros enters the nucleus of the GMC (Ikeshima-Kataoka *et al.,* 1997). In this way, Pros sub-cellular localisation allows the stem-cell-like properties of NBs to be maintained, while ensuring their GMC progeny do not adopt stem-cell-like characteristics, which would lead to overproliferation. However, the asymmetric segregation of Pros is not sufficient to account for its increased expression first in larval neurons (Carney *et al.,* 2013) and later in pupal NBs to stop proliferation (Maurange *et al.,* 2008).

The proliferation of all NBs, other than those leading to Mushroom body neurons, is terminated by a pulse of Pros expression and its entry into pupal NB nuclei. Elevated Pros drives the last NB division that leads to a pair of neurons (Maurange *et al.,* 2008). This final function of Pros is crucial for normal brain development, as it prevents overproliferation of the CNS (Kohwi and Doe, 2013; Maurange *et al.,* 2008). However, the mechanism that causes cell-type-specific up-regulation of Pros protein is poorly understood, despite its central importance in control NB proliferation.

Here, we elucidate the mechanism of up-regulation of Pros expression in larval neurons and terminal pupal NBs by adapting smFISH to work well in whole-mount brains. This method allows us to quantitate the levels of primary transcripts and cytoplasmic mRNA in individual cells at high temporal and spatial resolutions. We found that *pros* is transcribed at similar levels in NBs, GMCs and neurons, but its total RNA and protein level is significantly higher in new born larval neurons and pupal NBs that are in their final round of division. The burst of *pros* mRNA consists of an unusually long isoform of *pros* mRNA ($pros^{long}$) that contains a 15 kb 3' UTR. $pros^{long}$ is not transcribed in embryos nor in larval NBs, but is switched on in post-mitotic larval neurons and terminally dividing pupal NBs. We show that $pros^{long}$ is stabilised by binding to the conserved RNA-Binding Protein (RBP), Syncrip(Syp)/hnRNPQ (Liu *et al.,* 2015; McDermott *et al.,* 2014; Kuchler *et al.,* 2014). We show that $pros^{long}$ and Syp are both required to stop proliferation of terminal pupal NBs, by enabling a burst of Pros expression. Our observations highlight a novel mechanism of terminating stem cell division though transcription of a long isoform followed by regulated mRNA stability involving binding of a trans-acting factor to a long 3' UTR.

RESULTS

Up-regulation of Pros protein in neurons is achieved through post-transcriptional regulation

In order to examine cell-type-specific regulation of Pros expression, we first performed a careful analysis of antibody staining of Pros in the type I NB lineage. Pros is known to be localised in GMC nuclei, where it promotes GMC differentiation into neurons (Choksi *et al.,* 2006). We found that in addition to its expression in GMCs, Pros is up-regulated in new born neurons in comparison to NBs and GMCs (Figure 1A,B). To test whether the increase of Pros in immature larval neurons is achieved by an increase in primary transcription, we adapted smFISH methods (Buxbaum *et al.,* 2015) to work efficiently in whole-mount *Drosophila* larval brains. smFISH can be used to quantitate reliably the intensity of nuclear nascent transcript foci as a measure of primary transcription levels (Zenklusen *et al.,* 2008) in comparison to the levels of total *pros* mRNA and protein in the NBs and their progeny. NBs, GMCs and neurons were distinguished unambiguously using expression of an *asense-Gal4>mcD8::GFP* reporter that selectively marks type I NBs and GMCs, in combination with cell-type-specific markers as previously described (Figure S1, see methods for details). These stains identify the cells in the NB lineage definitively: NB express Asense (Ase) and Deadpan (Dpn), GMCs express Dpn only and neurons express Elav. We found that Pros protein expression correlates well with total *pros* mRNA levels, showing low expression in NBs and four-fold higher expression in neurons (Figure 1B,C,E,F). Unexpectedly, the level of *pros* primary transcription is similar in all cell types (Figure

1D,G), including in NBs, where both *pros* mRNA and Pros protein levels are significantly lower. Given that cytoplasmic *pros* mRNA levels were elevated in neurons, while the level of primary transcription was equal in all cells in the NB lineage, we conclude that the up-regulation of Pros protein in differentiating neurons depends on post-transcriptional mechanisms.

pros mRNA in larval brains contains an exceptionally long 3' UTR

Post-transcriptional regulation is often linked to expression of distinct alternative splicing or 3' UTR isoforms. Neurons have been shown to express transcript isoforms with unusually long 3'UTRs (Hilgers *et al.,* 2012; Hilgers *et al.,* 2011; Oktaba *et al.,* 2015). In FlyBase, *pros* is annotated as having six distinct isoforms with three different length 3' UTR*s*: ~1 kb, ~3 kb and ~15 kb (Figure 2A). In addition, previous publications showed that embryos only express a single ~6 kb *pros* RNA isoform corresponding to a 200 nt 3' UTR (Doe *et al.,* 1991; Vaessin *et al.,* 1991; Matsuzaki *et al.,* 1992). To test which isoforms are expressed in larval brains, we carried out Northern blots able to detect very long transcripts. Our Northern blot analysis using a probe that is common to all the annotated isoforms of *pros* transcripts (probe ALL), also detected a ~6 kb embryonic isoform (Figure 2A-B). The Northern blots also show that in larval brain extracts, there are multiple sized *pros* transcripts including approximately 6 kb, 9 kb and 21 kb in length (Figure 2B), corresponding to 3' UTR lengths of 200 nt, 3 kb and 15 kb, respectively. No band was found corresponding to the annotated 8 kb *pros* isoform containing a 1 kb 3' UTR. We also detected the 21 kb *pros* band in larval brains using a probe targeting a region that is unique to its predicted 15 kb 3' UTR.

The *pros* genomic sequence contains four possible canonical polyadenylation signals (PASs) downstream of the stop codons for all isoforms, corresponding to the four 3' UTR lengths discussed above. We tested the usage of these four PASs by sequencing the 3' end of RT-PCR clones generated using a primer that is specific to the upstream region of the predicted PAS and a generic oligo $(dT)_{15}$ primer (Davis and Ish-Horowicz, 1991). The sequencing results are consistent with the Northern blot data, indicating that polyadenylation occurs at positions leading to 3' UTRs 200 nt, 3 kb and 15 kb in length, corresponding to *pros* isoforms 6 kb, 9 kb and 21 kb in length, respectively (Figure S2). Considering all our results together, we conclude that embryos express only $pros^{very\text{-}short}$, containing a 3' UTR 200 nt in length, whereas larval brains contain two additional isoforms, $pros^{short}$ and $pros^{long}$, containing 3' UTRs 3 kb and 15 kb in length, respectively.

To investigate the patterns of expression of the three *pros* isoforms in larvae, we performed smFISH experiments using probes specific to the exonic 3 kb and 15 kb 3' UTR region of the *pros* transcript. $pros^{long}$, containing the 15 kb 3' UTR, is absent from NBs and GMCs and is only

expressed in neurons (Figure 2C. Figure S3). We compared *pros*^{long} and total *pros* primary transcription using smFISH with intron probes specific for the long isoform and against an intron that is common to all isoforms. We only detected transcription foci that are specific for the *pros*^{long} isoform in neurons and not in NBs and GMCs (Figure 2D). We conclude that the *pros*^{long} isoform is specifically transcribed in larval neurons.

To determine which *pros* isoform, *pros*$^{very\text{-}short}$ or *pros*^{short} is expressed in larval NBs and GMCs where the *pros*^{long} isoform is absent, we compared the signal intensity generated by the 3 kb 3' UTR probe, specific to *pros*^{short} and the exon probe common to both (Fig S3). If *pros*$^{very\text{-}short}$ is the predominant isoform, a higher signal is expected from the exon probe common to both isoforms. If *pros*^{short} is predominant, a similar signal level is expected from both probes. Our results show that similar signal was detected in NBs and GMCs from the *pros* exon and 3 kb 3' UTR. We conclude that *pros*^{short} with the 3 kb 3' UTR is most likely the predominant isoform in NBs and GMCs.

The *pros*^{long} isoform is required for the up-regulation of Pros protein in larval neurons and is stabilised by its 15kb 3' UTR

To test whether *pros*^{long} mRNA expression could account for the up-regulation of Pros protein in larval neurons, we first established whether the peaks of *pros* mRNA and protein occur in the same cells. We found a strong positive correlation (R^2=0.821) between expression levels of *pros*^{long} and Pros Protein (Figure 3A-B). To test directly whether the *pros*^{long} isoform is required for neuron-specific up-regulation of Pros expression, we created a mutation in the endogenous *pros* gene that specifically abolishes *pros*^{long} without affecting the expression of the other isoforms. The mutant introduces a stop codon in the unique N terminal protein coding region of the long isoform (*pros*$^{long\text{-}STOP}$) that causes the transcripts to be degraded by nonsense mediated mRNA decay (NMD) (Figure 3C and Materials and Methods). smFISH experiments confirm that *pros*^{long} mRNA is greatly reduced from the cytoplasm of *pros*$^{long\text{-}STOP}$ mutants despite being transcribed normally (Figure 3D-G), suggesting that the mutant transcripts are made but quickly degraded. Importantly, Pros protein levels are substantially reduced in *pros*$^{long\text{-}STOP}$ mutants and not up-regulated in neurons (Figure 3H-I). We conclude that *pros*^{long} is required for the cell-type-specific up-regulation of Pros protein in larval neurons.

To test whether the presence or absence of the extended 3' UTR of *pros* influences the abundance of *pros* mRNA, we constructed Green fluorescent protein (GFP) transgenes with either the 3 kb or 15 kb *pros* 3' UTR under *actin-gal-4* / UAS control (Figure 4A). Our results show that the presence of the 15 kb 3' UTR increases the stability of the transcript in the cytoplasm. We quantitated primary transcription and total mRNA of the two transgenes using

smFISH. The results showed that the presence of the long 15 kb 3' UTR did not affect transcription rate of the construct, but increased the level of cytoplasmic mRNA 5.75-fold (*p<0.001*) and of the resulting GFP protein 3.65-fold (*p<0.001*) relative to the short UTR reporter (Figure 4B-D). We conclude that the 15 kb 3' UTR of *pros* mRNA is sufficient to greatly increase transcript stability, although this does not exclude additional affects on translation efficiency. Together, these results show that larval neurons up-regulate Pros protein expression by specifically transcribing the $pros^{long}$ isoform, which is stabilised post-transcriptionally by the presence of its 15 kb 3' UTR.

The RNA-binding protein (RBP) Syp is expressed in the NB lineage, binds to pros mRNA and stabilises the $pros^{long}$ isoform

Post-transcriptional regulation in general and mRNA stability in particular depend on the action of specific RBPs. We previously showed that *pros* mRNA associates with Syp, a highly conserved RBP, in larval extracts (McDermott *et al.,* 2014). Mammalian SYNCRIP/hnRNPQ, is an important regulator of neural development (Liu *et al.,* 2015; Lelieveld *et al.* ,2016; Stoiber *et al.,* 2015), and has a number of post-transcriptional roles including regulating mRNA stability through binding at the 3' end of transcripts (Kuchler *et al.,* 2014; Kim *et al.,* 2011). For Syp to be a suitable candidate for regulating *pros* mRNA stability, it would have to be expressed and associated with *pros* mRNA in larval brains. We tested both these conditions and found that they are satisfied. Staining with an antibody against Syp, shows that the protein is highly enriched in the larval NBs and their progeny (Figure 5A). Immunoprecipitations (IPs) of *pros* mRNA using anti-Syp antibody shows that 58.3±4.5% of *pros* IPs with Syncrip in the larval brain, compared with negligible IP of the negative control *rp49* (Figure 5B,C). Moreover, IPs with IgG controls only pulled down a small fraction of both *pros* (1.10±0.83%) and *rp49* (0.97±0.54%) RNA. These results demonstrate that Syp binds strongly and specifically to *pros* RNA. Considering the presence of Syp in the NB lineage and its binding to *pros m*RNA, we conclude that Syp is a good candidate for an upstream regulator of *pros* mRNA stability.

To test whether Syp influences the levels of *pros* mRNA, we performed smFISH using *pros* exon and intron probes in *syp* mutant and wild-type brains. The results show that *pros* nascent transcripts levels are similar in both cases (Figure 5D,G) but total *pros* mRNA is significantly reduced in *syp* mutant compared to wild type (Figure 5E,G). Complementary biochemical methods confirmed these results using *pros* RT-qPCR on nuclear and cytoplasmic fractions of *syp* mutants and wild type brains (Figure S4 A-C and Methods). We also used quantitative smFISH to test whether the absence of cytoplasmic *pros* RNA in *syp* mutants is due to a defect

in nuclear mRNA export. *pros* mRNA is not retained in the nucleus in the absence of Syp (Figure S4 D-F).

We also compared Pros protein levels in wild type and *syp* mutant brains, which showed that the neuron specific Pros up-regulation is abolished in *syp* mutant (Figure 5F,G). We conclude that Syp mediates the up-regulation of Pros protein in neurons primarily by stabilising cytoplasmic *pros* mRNA, not by affecting the primary transcription or nuclear export of *pros* transcripts.

To test directly whether loss of cytoplasmic *pros* mRNA in *syp* mutants is due to the instability of the long isoform, we carried out transcriptomics analysis of *syp* mutant versus wild type brains. The results show that the abundance of $pros^{long}$ is specifically reduced in *syp* mutants, whereas the shorter *pros* forms are unaffected (Figure S5 A-B and Table S5). Northern blot analysis confirmed these findings, showing that the $pros^{long}$ isoform is reduced significantly in *syp* mutants whereas the abundance of the shorter *pros* isoforms remain unchanged (Figure 5H). We conclude that syp is required to specifically stabilise the long isoform of *pros*.

To test whether Syp is required for the activation of $pros^{long}$ transcription in neurons, we used an smFISH probe that is specific to the intron region of the $pros^{long}$ isoform. We found that the intensities of $pros^{long}$ primary transcription foci are the same in *syp* mutants and in wild type larvae (Figure S5 C-E). In contrast, cytoplasmic $pros^{long}$ mRNA as detected by smFISH probes specific to the long 3' UTR smFISH probe, is reduced significantly in *syp* mutants versus wild type. Taken together, our results show that transcriptional regulation of *pros* alone is not sufficient to produce the up-regulation peak of Pros expression observed in larval neurons. Therefore, we suggest that Syp regulates $pros^{long}$ stability post-transcriptionally.

We have demonstrated that both Syp and $pros^{long}$ are required to maintain high Pros protein level in larval neurons. We tested whether Syp and $pros^{long}$ are required to drive neuronal differentiation and to prevent neurons from reverting back to NBs, as is the case for some previously characterised mutants, such as *midlife crisis* (Carney *et al.,* 2013). We quantitated the number of NBs and their rate of proliferation in larvae of $pros^{long\text{-}STOP}$ and *syp* mutants and found no significant difference in NB numbers or mitotic index, compared to wild type. We used the NB specific anti-Deadpan (Dpn) antibody, and anti-Phospho-Histone3 (PH3) antibody to identify and mark mitotic NBs (Figure 6A,C-D). We conclude that $pros^{long}$, is not required to maintain larval neurons in a differentiated state, nor to control the rate of larval NB proliferation.

pros^{long} is essential for pupal NBs to exit division

A burst of Pros expression is known to have an important role in terminating NB divisions in pupae. To test whether Syp or *pros^{long}* also have a role in terminating pupal NB division, we quantitated NBs in *syp* and *pros$^{long\text{-}STOP}$* mutant pupal brains compared with wild type. We found that in *syp* and *pros$^{long\text{-}STOP}$* mutant NBs continue to divide, when NBs in wild type brains have already terminated. As previously published, we found that 48 hours after pupal formation (APF), in wild type pupal brains there are only 4 mushroom body NBs remaining in each hemisphere, while all other NBs have undergone terminal symmetric division to produce two neurons (Siegrist *et al.,* 2010). In contrast, in both *syp* and *pros$^{long\text{-}STOP}$* pupal brains, we found a large number of NBs remain and there is no significant change in mitotic index from the wild type larva, suggesting that these long-lived NBs continue to divide at the same rate (Figure 6B,C-D). In addition, we observed a significant number of PH3^{+} Dpn^{-} cells adjacent to these long-living NBs in *syp* and *pros$^{long\text{-}STOP}$* mutants (yellow arrows, Figure 6B). These cells are likely to be GMCs produced by the remaining NBs through regular asymmetric division. We conclude Syp and *pros^{long}* are required for the termination of NB division in pupae.

Previous work showed that termination of pupal NBs division requires a transient up-regulation of Pros protein and that expression of transgenic Pros can terminate NBs at any stage (Maurange *et al.,* 2008). To test whether a transient up-regulation of Pros in pupal NBs is achieved by the activation of *pros^{long}* isoform transcription and subsequent transcript stabilisation by Syp, we performed smFISH with intron probes that are specific to the *pros^{long}* isoform in conjunction with Dpn and Pros protein staining. In wild type pupal brains, we found that such transient nuclear Pros up-regulation in terminal pupal NBs correlates with the activation of *pros^{long}* transcription (Figure 7A,E). In contrast, in pupal NBs that lack *pros^{long}* mRNA, Pros protein level remains low (Figure 7B,E). In *syp* mutant pupal NBs, *pros^{long}* mRNA is transcribed, but Pros protein fails to up-regulate, apparently due to failure of *pros^{long}* mRNA to be stabilised in the absence of Syp (Figure 7C-D,E). Taking all our results together, we conclude that in pupae, NBs activate transcription of *pros^{long}* and the transcript is stabilised by Syp binding to the 15 kb 3' UTR. Therefore, *pros^{long}* expression and stabilisation lead to the transient up-regulation of Pros protein that drives the final symmetric division of pupal NBs.

DISCUSSION

Many key regulators of NB proliferation and differentiation, in particular transcription factors (TFs), have now been identified and characterised (Kambadur *et al.,* 1998; Isshiki *et al.,* 2001; Novotny *et al.,* 2002; Pearson and Doe, 2003; Grosskortenhaus *et al.,* 2006; Li *et al.,* 2013; Narbonne-Reveau *et al.,* 2016; Kohwi and Doe, 2013). A general consensus has emerged in the field for both *Drosophila* and mammals, namely that a temporal sequence of TFs is predominantly responsible for controlling the gene expression landscape that governs NB proliferation and differentiation. Our use of quantitative smFISH methods opens up the possibility of addressing conclusively the roles of primary transcription and post-transcriptional regulation at an individual cell level within the intact brain. We have highlighted how a key aspect of the expression and function of the TF Pros is regulated by the stability of its long mRNA isoform ($pros^{long}$). These findings suggest that multiple, hitherto unappreciated layers of post-transcriptional regulation are likely to be important for regulating other aspects of stem cell proliferation and differentiation. Indeed, the generality of our findings is supported by the fact that many genes that function in the brain have complex gene structures such as multiple isoforms and long 3' UTRs, hallmarks of post-transcriptional mechanisms (Stoiber *et al.,* 2015; Hilgers *et al.,* 2011; Tekotte *et al.,* 2002; Berger *et al.,* 2012).

Post-transcriptional and transcriptional regulation work hand-in-hand to achieve cell specific gene expression

Our experiments show that $pros^{long}$ is selectively transcribed in larval neurons and in terminally dividing pupal NBs. It is currently unclear what induces the activation of this tissue specific pulse of $pros^{long}$ transcription, but we show that once transcribed, the presence of $pros^{long}$ is regulated through an exceptionally long 15 kb 3' UTR, which is stabilised by Syp. The use of long 3' UTRs has been widely described in other biological contexts (Yeh and Yong, 2016; Hilgers, 2015). Moreover, gene specific 3' UTR extension has been reported during *Drosophila* embryonic neurogenesis (Hilgers *el al.,* 2011; Smibert *et al.,* 2012; Oktaba *et al.,* 2015). In the case of *pros*, we have demonstrated a functional role for its long 3' UTR in stabilising $pros^{long}$, required for NB termination. We hypothesise that the functional role of 3' UTR extension will also be important for other prominent examples of *Drosophila* neural genes with annotated extended 3' UTR isoforms. These include the regulator of the timing of neuronal development, Chinmo (Liu *et al.,* 2015), and the mRNA-binding proteins with important roles in post-transcriptional regulation and NB biology, Brat (Bello *et al.,* 2006; Betschinger *et al.,* 2006; Lee *et al.,* 2006) and Imp (Liu *et al.,* 2015), all of which have complex isoform structures. Therefore, our data in the context of previous studies suggest a general principle of post-transcriptional regulation of the expression

of many key neuronal transcripts, through cell-type specific presence of isoforms with distinct 3' UTRs.

Previous work has shown that the loss of Pros in larval neurons is not sufficient to lead to their de-differentiation back to NBs (Carney *et al.,* 2013). In agreement with these observations, we found that *pros*$^{long\text{-}STOP}$ mutants also do not cause neurons to de-differentiate into NBs. We interpret these observations as indicating that *pros*^{long} has no essential role in the differentiation of neurons. Instead, *pros*^{long} mRNA stabilisation is specifically required in pupal NBs to terminate their divisions by boosting the expression of Pros at a particular place, time and cell type in development. Therefore, *pros*^{long} mRNA stability is regulated hand-in-hand with the choice of which *pros* isoform is transcribed, to enable the uncoupling of low level Pros expression required for neuronal differentiation from a specific burst of Pros expression needed to terminate NB division. In addition, the dependence of *pros*^{long}, but not the shorter *pros* isoforms, on Syp for its stabilisation, allows further separation of control of *pros*^{long} levels from those of the other isoforms.

Regulating expression levels by differential mRNA isoform stability and long 3' UTRs is likely to be a conserved mechanism

Although regulated mRNA stability has not been well characterised mechanistically in neural stem cells, there are many examples of unstable mRNAs in a variety of biological and medical contexts (Ulitsky *et al.,* 2012; Miura *et al.,* 2014). For example, regulated mRNA stability is very common during the early embryonic development of *Drosophila* (Chen *et al.,* 2014; Laver *et al.,* 2015). Moreover, in single cell models, including yeast, *Drosophila* S2 cells and mammalian tissue culture cells, mRNA stability is known to play many varied and important roles (Chávez *et al.,* 2016; Sin and Nollen, 2015; Forrest and Khalil, 2017; Moszyńska *et al.,* 2017; Maeda and Akira, 2017) and often involves isoforms with distinct 3' UTRs (Catalan *et al.,* 2016; Hopkins *et al.,* 2016; Mitra *et al.,* 2015). More generally, post-transcriptional mechanisms are thought to be essential for many neuronal functions, ranging from synaptic plasticity (Capitano *et al.,* 2017; Lee *et al.,* 2015) to neurodegeneration (Cookson, 2017; Tang, 2016; Kim *et al.,* 2011; Nussbacher *et al.,* 2015) and neurological diseases (Wang *et al.,* 2016). Therefore, we anticipate that regulated mRNA stability and the use of isoforms with distinct 3' UTRs will also play major and wide-spread roles in both vertebrate and invertebrate stem cell biology, especially in the nervous system.

Drosophila and mammals share many molecular mechanisms driving nervous system development. We propose that the post-transcriptional mechanisms we have uncovered are also conserved in mammals. Certainly, Prox1, the mammalian TF orthologue of Pros, is a

tumour suppressor that regulates stem cell differentiation in the brain as well as many other organ systems (Stergiopoulos *et al.,* 2015; Elsir *et al.,* 2012). Like *pros*, *prox1* also has several isoforms including one containing a long 3' UTR. Furthermore, a burst of Prox1 expression is required to drive the differentiation of immature granular neurons in the adult hippocampus (Hsieh, 2012). It is also likely that post-transcriptional regulation by RBPs helps determine the expression and translatability of Prox1. Future experiments will have to discover whether Prox1 expression, like *pros,* is regulated through stabilisation of its 3' UTR in order to terminate neural stem cell proliferation.

Our newly established quantitative application of smFISH to the *Drosophila* brain enables a new level of characterisation of post-transcriptional regulation mechanisms, also in other systems. Indeed, there is increasing evidence that RNA-binding proteins play critical roles in *Drosophila* and mammalian brain development (Stoiber *et al.* 2015; Berger *et al.,* 2012; Neumuller *et al.,* 2011; Bryant *et al.,* 2016), and that their dysfunction is associated with neurological disease (Nussbacher *et al.,* 2015). We expect that applying smFISH in mammalian models will transform studies of the regulation of gene expression in complex tissues.

AUTHOR CONTRIBUTIONS

Lu Yang (L.Y.) - Conception of project, the majority of the experimental work including a contribution to genome wide analysis, data analysis and interpretation, initial draft of the manuscript and involvement in its revision.

Tamsin J. Samuels (T.J.S.) – Syncrip and IgG immunoprecipitation experiments, RNA sequencing and data analysis as well as involvement in revising the manuscript.

Yoav Arava (Y.A.) – Northern blots.

Francesca Robertson (F.R.) – Guidance and advice on CrispR, Bac cloning.

Aino I. Järvelin (A.I.J.) – Bioinformatics and data visualization for RNA sequence data.

Ching-Po Yang (C.P.Y.) – Advice and guidance on phenotypic analysis.

Tzumin Lee (T.L.) – Guidance on data interpretation and phenotypic analysis experimental design, comments on the manuscript.

David Ish-Horowicz (D.I.H.) - Guidance of the project to completion and manuscript revision.

Ilan Davis (I.D.) – Conception of project and its guidance to completion, data analysis and its interpretation and writing of the manuscript.

ACKNOWLEDGEMENTS

We are grateful to Andrew Bassett (Genome Engineering Oxford, GEO) for assistance in designing and validating CrispR guide RNAs, Tomek Dobrzycki for initial work that lead to the project, Alan Wainman and Richard M. Parton for advice on advanced microscopy, Darragh Ennis for help and advice with fly husbandry and administration. We are also indebted to Wolfgang Rau, Alfredo Castello, Lidia Vasilieva, Jordan Raff and Neil Brockdorff for comments on the manuscript. We would also like to thank, the Cambridge Fly Facility for transgenic production, the Bloomington *Drosophila* Stock Centre, P[acman] Resources. L.Y. was funded from the Clarendon Trust and Goodger Fund., T.J.S. was funded by Wellcome Trust Four-Year PhD Studentship (105363/Z/14/Z), F.R. was funded by a Marie Curie Postdoctoral Fellowship. C.P.Y. and T.L. were supported by Howard Hughes Medical Institute. D.I.H. was funded by University College London. I.D. was funded from a Wellcome Senior Research Fellowship (081858), which also supported A.I.J., MICRON Oxford (http://micronoxford.com, supported by a Wellcome Strategic Awards to ID (091911/B/10/Z and 107457/Z/15/Z) providing access to equipment and advice on advanced imaging techniques.

REFENRENCES

Bassett, A., Liu, J.L., (2014). CRISPR/Cas9 mediated genome engineering in Drosophila. *Methods*. **69**, 128–136.

Bayraktar, O. A., Boone, J. Q., Drummond, M. L., Doe, C. Q., (2010). *Drosophila* type II neuroblast lineages keep Prospero levels low to generate large clones that contribute to the adult brain central complex. *Neural Development,* 5(26)

Bello, B., Reichert, H., & Hirth, F., (2006). The brain tumor gene negatively regulates neural progenitor cell proliferation in the larval central brain of Drosophila. *Development*, *133*(14), 2639–2648.

Berger, C., Harzer, H., Burkard, T. R., Steinmann, J., van der Horst, S., Laurenson, A.S., Novatchkova, M., Reichert, H., Knoblich, J. A., (2012). FACS purifcation and transcriptome analysis of drosophila neural stem cells reveals a role for Klumpfuss in self-renewal. *CellReports*, *2*(2), 407–418.

Betschinger, Joerg, Mechtler, K., & Knoblich, J. A., (2006). Asymmetric segregation of the tumor suppressor brat regulates self-renewal in Drosophila neural stem cells. *Cell*, *124*(6), 1241–1253.

Bryant, C. D. & Yazdani, N., (2016). RNA binding proteins, neural development and the addictions. *Genes Brain Behav,* 15(1), 169-186.

Buxbaum, A. R., Haimovich, G. & Singer, R. H., (2015). In the right place at the right time: visualizing and understanding mRNA localization. *Nature Reviews Molecular Cell Biology*, 16(2), pp.95–109.

Capitano, F., Camon, J., Licursi, V., Ferretti, V., Maggi, L., Scianni, M., Del Vecchio, G., Rinaldi, A., Mannironi, C., Limatola, C., Presutti, C., Mele, A., (2017). MicroRNA-335-5p modulates spatial memory and hippocampal synaptic plasticity. *Neurobiology of Learning and Memory*, 139, pp.63–68.

Carney, T. D., Struck, A. J., & Doe, C. Q., (2013). midlife crisis encodes a conserved zinc-finger protein required to maintain neuronal differentiation in Drosophila. *Development*, *140*(20), 4155–4164.

Catalan, A., Glaser-Schmitt, A., Argyridou, E., Duchen, P., Parsch, J., (2016). An indel polymorphism in the MtnA 3' untranslated region is associated with gene expression variation and local adaptation in *Drosophila melanogaster*. *PLOS Genetics*, 12(4): e1005987

Chávez, S., Garcia-Martinez, J., Delgado-Ramos, L., Perez-Ortin, J. E., (2016). The importance of controlling mRNA turnover during cell proliferation. *Current genetics*, 62(4), pp.701–710.

Chen, L., Dumelie, J. G., Li, X., Cheng, M. H., Yang, Z., Laver, J. D., Siddiqui, N. U., Westwood, J. T., Morris, Q., Lipshitz, H. D., Smibert, C. A., (2014). Global regulation of mRNA translation and stability in the early *Drosophila* embryo by the Smaug RNA-binding protein. *Genome Biology*, 15(1), p.R4.

Choksi, S. P., Southall, T. D., Bossing, T., Edo , K., de Wit, E., Fischer, B. E., van Steensel, B., Micklem, G., Brand, A. H., (2006). Prospero acts as a binary switch between self-renewal and differentiation in Drosophila neural stem cells. *Developmental Cell*, *11*(6), 775–789.

Cookson, M. R., (2017). RNA-binding proteins implicated in neurodegenerative diseases. *Wiley Interdisciplinary Reviews: RNA*, 8(1), p.e1397.

Davis, I., & Ish-Horowicz, D., (1991). Apical localization of pair-rule transcripts requires 3' sequences and limits protein diffusion in the Drosophila blastoderm embryo. *Cell*, *67*(5), 927–940.

Doe, C. Q., Chu-LaGra , Q., Wright, D. M., & Scott, M. P., (1991). The prospero gene specifies cell fates in the Drosophila central nervous system. *Cell*, *65*(3), 451–464.

Dyer, M. A., (2002). Regulation of proliferation, cell fate specification and differentiation by the homeodomain proteins Prox1, Six3, and Chx10 in the developing retina. *Cell cycle* 2(4), 350-7

Elsir, T., Smits, A., Lindström, M. S., & Nistér, M., (2012). Transcription factor PROX1: its role in development and cancer. *Cancer and Metastasis Reviews*, *31*(3-4), 793–805.

Forrest, M. E. & Khalil, A. M., (2017). Review: Regulation of the cancer epigenome by long non-coding RNAs. *Cancer Letters*.

Foskolou, I. P., Stellas, D., Rozani, I., Lavigne, M. D., Politis, P. K., (2013). Prox1 suppresses the proliferation of neuroblastoma cells via a dual action in p27-Kip1 and Cdc25A. *Oncogene*, 32(8), pp.947–960.

Gramates L. S., Marygold, S. J., dos Santos, G., Urbano, J. M., Antonazzo, G., Matthews, B. B., Rey, A. J., Tabone, C. J., Crosby, M. A., Emmert, D. B., et al., (2017). FlyBase at 25: looking to the future. *Nucleix Acids Res,* 45(D1):D663-D671

Grosskortenhaus, R., Robinson, K. J., Doe, C. Q., (2006). Pdm and Castor specify late-born motor neuron identity in the NB7-1 lineage. *Genes Dev.* 20(18), 2618-2627

Hilgers, V., (2015). Alternative polyadenylation coupled to transcription initiation: Insights from ELAV-mediated 3' UTR extension. *RNA Biology*, 12(9), pp.918–921.

Hilgers, V., Perry, M. W., Hendrix, D., Stark, A., Levine, M., & Haley, B., (2011). Neural-specific elongation of 3' UTRs during Drosophila development. *Proceedings of the National Academy of Sciences of the United States of America*, *108*(38), 15864–15869.

Hilgers, V., Lemke, S. B. & Levine, M., (2012). ELAV mediates 3' UTR extension in the *Drosophila* nervous system. *Genes & Development*, 26(20), pp.2259–2264.

Hirata, J., Nakagoshi, H., Nabeshima, Y., & Matsuzaki, F., (1995). Asymmetric segregation of the homeodomain protein Prospero during Drosophila development. *Nature*, *377*(6550), 627–630.

Homem, C. C. F., & Knoblich, J. A., (2012). Drosophila neuroblasts: a model for stem cell biology. *Development*, *139*(23), 4297–4310.

Hopkins, T. G., Mura, M., Al-Ashtal, H. A. and Lahr, R. M., (2016) 'The RNA-binding protein LARP1 is a post-transcriptional regulator of survival and tumorigenesis in ovarian cancer'. *Nucleic acids Res,* 44(3), 1227-1246.

Hsieh, J., (2012). Orchestrating transcriptional control of adult neurogenesis. *Genes & Development*, 26(10), pp.1010–1021.

Ikeshima-Kataoka, H., Skeath, J. B., Nabeshima, Y., Doe, C. Q., & Matsuzaki, F., (1997). Miranda directs Prospero to a daughter cell during Drosophila asymmetric divisions. *Nature*, *390*(6660), 625–629.

Isshiki, T., Pearson, B., Holbrook, S., & Doe, C. Q., (2001). Drosophila neuroblasts sequentially express transcription factors which specify the temporal identity of their neuronal progeny. *Cell*, *106*(4), 511–521.

Kambadur, R., Koizumi, K., Stivers, C., Nagle, J., Poole, S. J., & Odenwald, W. F., (1998). Regulation of POU genes by castor and hunchback establishes layered compartments in the Drosophila CNS. *Genes & Development*, *12*(2), 246–260.

Kato, K., Konno, D., Berry, M., Matsuzaki, F., Logan, A., Hidalgo, A., (2015). Prox1 Inhibits Proliferation and Is Required for Differentiation of the Oligodendrocyte Cell Lineage in the Mouse F. de Castro, ed. *PLoS ONE*, 10(12), p.e0145334.

Kelava, I. & Lancaster, M.A., (2016). Stem Cell Models of Human Brain Development. *Cell stem cell*, 18(6), pp.736–748.

Kim, D., Pertea, G., Trapnell, C., Pimentel, H., Kelley, R., Salzberg, S. L., (2013). TopHat2: accurate alignment of transcriptomes in the presence of insertions, deletions and gene fusions. *Genome Biology*, 14(4), p.R36.

Kim, D. Y., Kwak, E., Kim, S. H., Lee, K. H., Woo, K. C., Kim, K. T., (2011). hnRNP Q mediates a phase-dependent translation-coupled mRNA decay of mouse Period3. *Nucleic acids research*, 39(20), pp.8901–8914.

Kitajima, A., Fuse, N., Isshiki, T., Matsuzaki, F., (2010). Progenitor properties of symmetrically dividing *Drosophila* neuroblasts during embryonic and larval development. *Developmental Biology*, 347(1), pp.9–23.

Knoblich, J. A., (2008). Mechanisms of asymmetric stem cell division. *Cell*, *132*(4), 583–597.

Knoblich, J A, Jan, L. Y., & Jan, Y. N., (1995). Asymmetric segregation of Numb and Prospero during cell division. *Nature*, *377*(6550), 624–627.

Kohwi, M. & Doe, C. Q., (2013). Temporal fate specification and neural progenitor competence during development. *Nat Rev Neurosci,* 14(12), 823-38.

Kuchler, L., Giegerich, A. K., Sha, L. K., Knape, T., Wong, M. S., Schröder, K., Brandes, R. P., Heide, H., Wittig, I., Brune, B., von Knethen, A., (2014). SYNCRIP-dependent Nox2 mRNA destabilization impairs ROS formation in M2- polarized macrophages. *Antioxidants & Redox Signaling*, *21*(18), 2483–2497.

Lai, S. L., & Doe, C. Q., (2014). Transient nuclear Prospero induces neural progenitor quiescence. *eLife*, *3*, 379.

Laver, J. D., Li, X., Ray, D., Cook, K. B., Hahn, N. A., Nabeel-Shah, S., et al., (2015). Brain tumor is a sequence-specific RNA-binding protein that directs maternal mRNA clearance during the Drosophila maternal-to-zygotic transition. *Genome Biology*, *16*(1), 94.

Lee, C. Y., Wilkinson, B. D., Siegrist, S. E., Wharton, R. P., & Doe, C. Q., (2006). Brat is a Miranda cargo protein that promotes neuronal differentiation and inhibits neuroblast self-renewal. *Developmental Cell*, *10*(4), 441–449.

Lee, Y. S., Lee, J. A. & Kaang, B. K., (2015). Regulation of mRNA stability by ARE-binding proteins in synaptic plasticity and memory. *Neurobiology of Learning and Memory*, 124, pp.28–33.

Lelieveld, S. H., Reijnders, M. R. F., Pfundt, R., Yntema, H. G., Kamsteeg, E. J., de Vries, P., de Vries, B. B. A., Willemsen, M. H., Kleefstra, T., Lohner, K., et al., (2016). Meta-analysis of 2,104 trios provides support for 10 new genes for intellectual disability. *Nature Neuroscience*, 19(9), pp.1194–1196.

Li, X., Erclik, T., Bertet, C., Chen, Z., Voutev, R., Venkatesh, S., Morante, J., Celik, A., Desplan, C., (2013). Temporal patterning of *Drosophila* medulla neuroblasts controls neural fates. *Nature*, 498(7455), pp.456–462.

Liu, Z., Yang, C. P., Sugino, K., Fu, C. C., Liu, L. Y., Yao, X., Lee, L. P., Lee, T., (2015). Opposing intrinsic temporal gradients guide neural stem cell production of varied neuronal fates. *Science*, *350*(6258), 317–320.

Livak, K. J., & Schmittgen, T. D., (2001). Analysis of relative gene expression data using real- time quantitative PCR and the 2(-Delta Delta C(T)) Method. *Methods*, *25*(4), 402–408.

Love, M.I., Huber, W. & Anders, S., (2014). Moderated estimation of fold change and dispersion for RNA-seq data with DESeq2. *Genome Biology*, 15(12), p.550.

Maeda, K. & Akira, S., (2017). Regulation of mRNA stability by CCCH-type zinc-finger proteins in immune cells. *International immunology*.

Matsuzaki, F., Koizumi, K., Hama, C., Yoshioka, T., & Nabeshima, Y., (1992). Cloning of the Drosophila prospero gene and its expression in ganglion mother cells. *Biochemical and Biophysical Research Communications*, *182*(3), 1326–1332.

Maurange, C., Cheng, L., & Gould, A. P., (2008). Temporal transcription factors and their targets schedule the end of neural proliferation in Drosophila. *Cell*, *133*(5), 891–902.

McDermott, S. M., Meignin, C., Rappsilber, J., Davis, I., (2012). *Drosophila* Syncrip binds the *gurken* mRNA localisation signal and regulates localised transcripts during axis specification. *Biology Open,* 1, 488-497.

McDermott, S. M., Yang, L., Halstead, J. M., Hamilton, R. S., Meignin, C., & Davis, I., (2014). Drosophila Syncrip modulates the expression of mRNAs encoding key synaptic proteins required for morphology at the neuromuscular junction. *RNA*, *20*(10), 1593–1606.

Mitra, M., Johnson, E. L. and Coller, H. A., (2015) 'Alternative polyadenylation can regulate post-translational membrane localization.', *Trends in cell & molecular biology*. NIH Public Access, 10, pp. 37–47.

Miura, P., Sanfilippo, P., Shenker, S., Lai, E. C., (2014). Alternative polyadenylation in the nervous system: To what lengths will 3′ UTR extensions take us? *BioEssays*, 36(8), pp. 766–777.

Moszyńska, A. Gebert, M., Collawn, J. F., Bartoszewski, R., (2017). SNPs in microRNA target sites and their potential role in human disease. *Open biology*, 7(4), p.170019.

Narbonne-Reveau, K., Lanet, E., Dillard, C., Foppolo, S., Chen, C. H., Parrinello, H., Rialle, S., Sokol, N. S., Maurange, C., (2016). Neural stem cell-encoded temporal patterning delineates an early window of malignant susceptibility in *Drosophila*. *eLife*, 14(5), p.e13463.

Neumuller, R. A., Richter, C., Fischer, A., Novatchkova, M., Neumuller, K.G., Knoblich, J. A., (2011). Genome-wide analysis of self-renewal in *Drosophila* neural stem cells by transgenic RNAi. *Cell Stem Cell.* 8(5), 580,593.

Novotny, T., Eiselt, R., & Urban, J., (2002). Hunchback is required for the specification of the early sublineage of neuroblast 7-3 in the Drosophila central nervous system. *Development*, *129*(4), 1027–1036.

Nussbacher, J.K., Batra, R., Lagier-Tourenne, C., Yeo, G. W., (2015). RNA-binding proteins in neurodegeneration: Seq and you shall receive. *Trends in neurosciences*, 38(4), pp. 226–236.

Oktaba, K., Zhang, W., Lotz, T. S., Jun, D. J., Lemke, S. B., Ng, S. P., Esposito, E., Levine, M., Holgers, V., (2015). ELAV links paused Pol II to alternative polyadenylation in the Drosophila nervous system. *Molecular Cell*, *57*(2), 341–348.

Pearson, B. J., & Doe, C. Q., (2003). Regulation of neuroblast competence in Drosophila. *Nature*, *425*(6958), 624–628.

Siegrist, S. E., Haque, N. S., Chen, C. H., Hay, B. A., Hariharan, I. K., (2010). Inactivation of both Foxo and reaper promotes long-term adult neurogenesis in Drosophila. *Curr. Biol*. 20, 643-648.

Sin, O. & Nollen, E.A.A., (2015). Regulation of protein homeostasis in neurodegenerative diseases: the role of coding and non-coding genes. *Cellular and Molecular Life Sciences*, 72(21), pp.4027–4047.

Smibert, P., Miura, P., Westholm, J. O., Shenker, S., May, G., Du , M. O., et al., (2012). Global patterns of tissue-specific alternative polyadenylation in Drosophila. *CellReports*, *1*(3), 277–289.

Spana, E.P. & Doe, C.Q., (1995). The prospero transcription factor is asymmetrically localized to the cell cortex during neuroblast mitosis in *Drosophila*. *Development*, 121(10), pp.3187–3195.

Stergiopoulos, A., Elkouris, M. & Politis, P.K., (2015). Prospero-related homeobox 1 (Prox1) at the crossroads of diverse pathways during adult neural fate specification. *Frontiers in Cellular Neuroscience*, 8, p.10484.

Stoiber, M. H., Olson, S., May, G. E., Du , M. O., Manent, J., Obar, R., Guruharsha, K. G., Bickel, P. J., Artavanis-Tsakonas, S., Brown, J. B., et al., (2015). Extensive cross-regulation of post-transcriptional regulatory networks in Drosophila. *Genome Research*, *25*(11), 1692–1702.

Tang, A.Y., (2016). RNA processing-associated molecular mechanisms of neurodegenerative diseases. *Journal of applied genetics*, 57(3), pp.323–333.

Tekotte, H., Berdnik, D., Torok, T., Buszczak, M., Jones, L. M., Cooley, L., Knoblich, J. A., Davis, I., (2002). Dcas Is Required for importin-α3 Nuclear Export and Mechano-Sensory Organ Cell Fate Specification in *Drosophila*. *Developmental Biology*, 244(2), pp.396–406.

Trcek, T., Larson, D.R., Moldón, A., Query, C.C., Singer, R.H., (2011). Single-Molecule mRNA Decay Measurements Reveal Promoter- Regulated mRNA Stability in Yeast. *Cell*, 147(7), pp.1484–1497.

Ulitsky, I., Shkumatava, A., Jan, C. H., Subtelny, A. O., Koppstein, D., Bell, G. W., Sive, H., Bartel, D. P., (2012). Extensive alternative polyadenylation during zebrafish development. *Genome Res,* 22(10), 2054-66

Vaessin, H., Grell, E., Wol , E., Bier, E., Jan, L. Y., & Jan, Y. N., (1991). prospero is expressed in neuronal precursors and encodes a nuclear protein that is involved in the control of axonal outgrowth in Drosophila. *Cell*, *67*(5), 941–953.

Venken, K.J.T., He, Y., Hoskins, R.A., Bellen, H.J., (2006). P[acman]: A BAC Transgenic Platform for Targeted Insertion of Large DNA Fragments in *D. melanogaster. Science*, 314(5806), pp.1747–1751.

Wang, E.T., Taliaferro, J. M., Lee, J. A., Sudhakaran, I. P., Rossoll, W., Gross, C., Moss, K. R., Bassell, G. J., (2016). Dysregulation of mRNA Localization and Translation in Genetic Disease. *Journal of Neuroscience*, 36(45), pp.11418–11426.

Yeh, H.S., Yong, J., (2016). Alternative Polyadenylation of mRNAs: 3′-Untranslated Region Matters in Gene Expression. *Molecules and cells*, 39(4), pp.281–285.

Zenklusen, D., Larson, D.R. & Singer, R.H., (2008). Single-RNA counting reveals alternative modes of gene expression in yeast. *Nature structural & molecular biology*, 15(12), pp. 1263–1271.

Zhu, S., Lin, S., Kao, C.-F., Awasaki, T., Chiang, A.-S., & Lee, T., (2006). Gradients of the Drosophila Chinmo BTB-zinc nger protein govern neuronal temporal identity. *Cell*, *127*(2), 409–422.

FIGURES

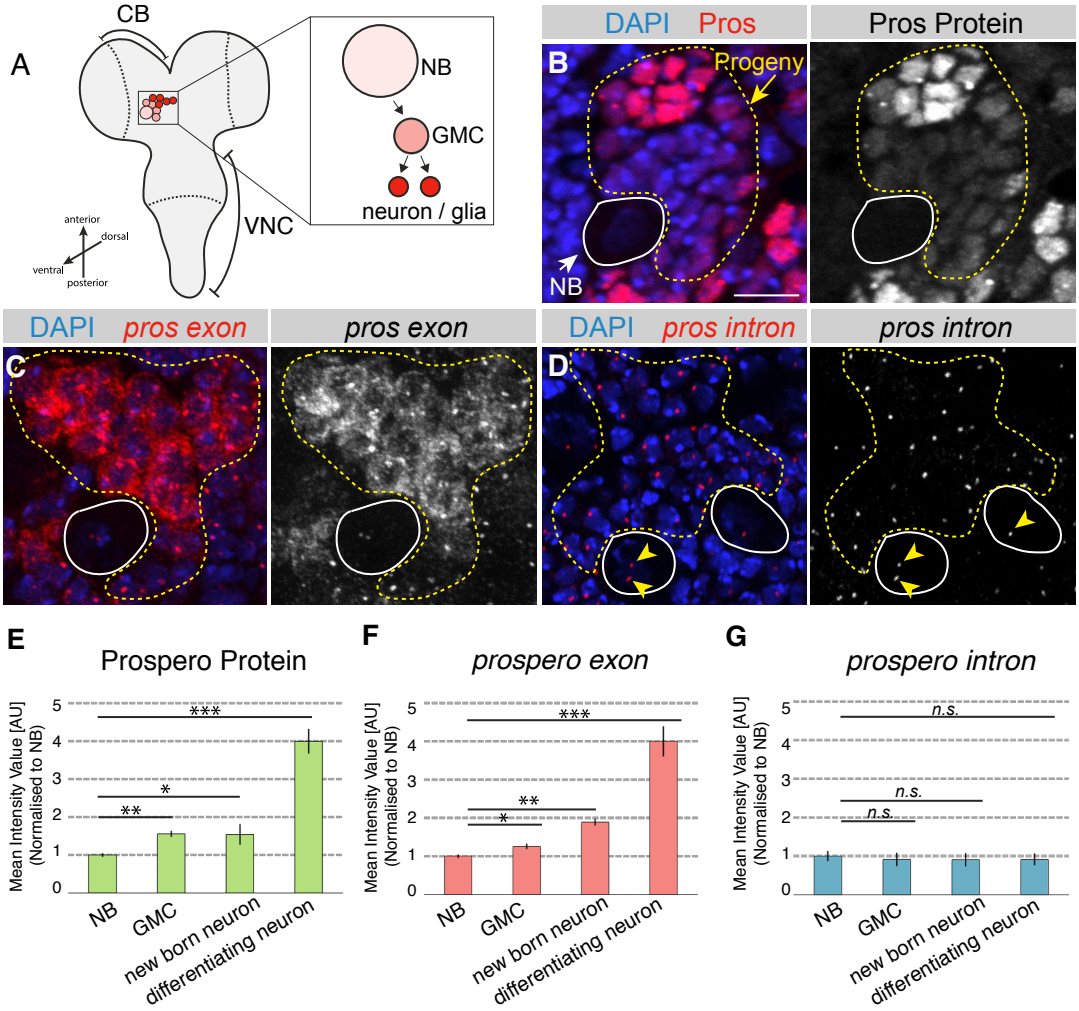

Figure 1: Pros cell-type-specific expression is regulated post-transcriptionally

(A) Prospero (Pros) protein expression level in type I neuroblasts (NBs) and progeny. **(B-D)** Pros immunofluorescence and *pros* exon and intron single molecule fluorescent *in situ* hybridisation (smFISH) showing Pros protein **(B)** and mRNA level **(C)** increases as NB progeny mature but *pros* mRNA is transcribed at a similar level in all cell types (**D**), even in NBs where there are low levels of Pros protein and *pros* mRNA (yellow arrow). **(E-G)** Quantification of Pros protein, total *pros* mRNA and *pros* nascent transcripts in NBs, ganglion mother cells (GMCs), new born neurons and differentiating neurons. Asense-driven mCD8::GFP fluorescence intensity was used as an indicator of NB progeny age (See Figure S1). In this and all subsequent figures, 3 clusters in each of 3 brains were analyses. Error bars represent SEM. *$p \leq 0.05$, **$p \leq 0.01$, ***$p < 0.001$, *n.s. = not significant.* Scale bar: 10 μm (unless otherwise stated).

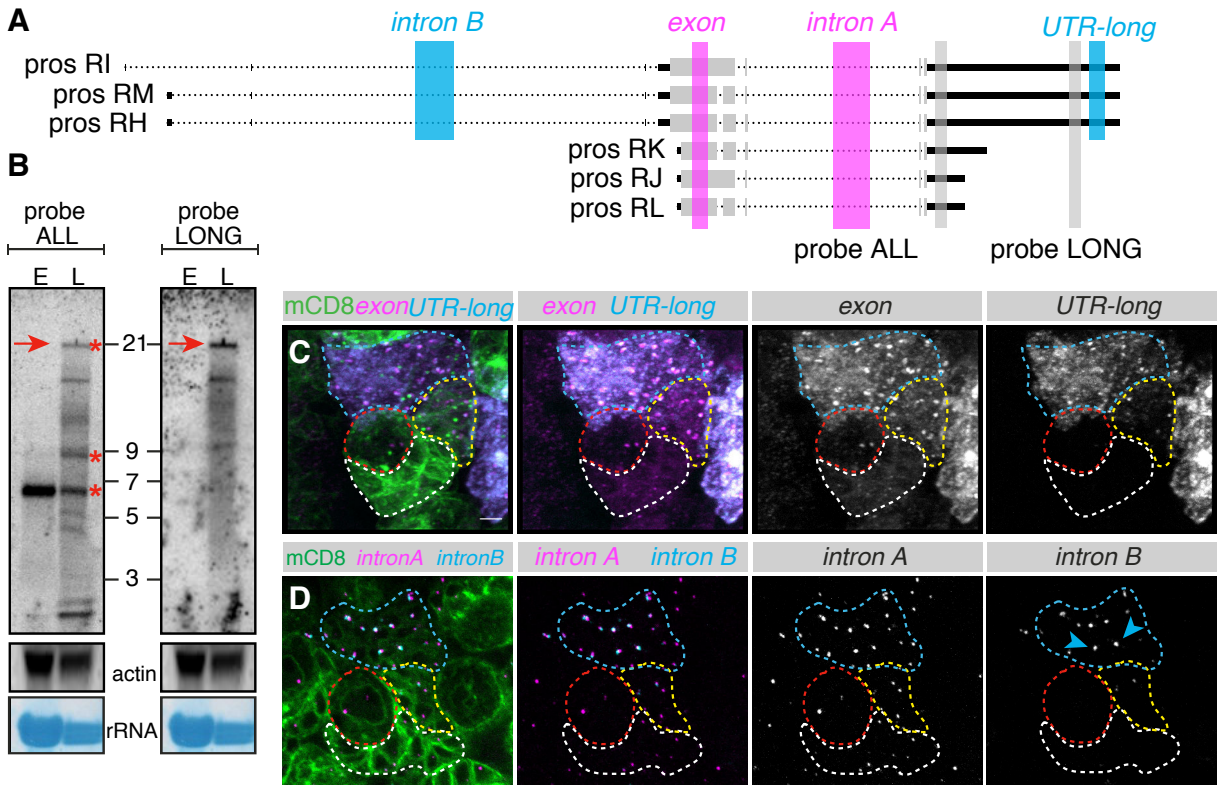

Figure 2: *pros*^{long} isoform is expressed post-embryonic stage and is specifically transcribed in larval neurons

(A) Diagram showing six annotated *pros* transcript isoforms and the position of smFISH (magenta bars recognising all isoforms and blue bars specific to *pros*^{long}) and Northern blot probes (grey bars). **(B)** Northern blot confirms the existence of multiple *pros* mRNA isoforms at 6 kb, 9 kb and 21 kb (red asterisk) in the larval central nervous system (CNS). The 21 kb isoform corresponds to *pros* transcript with 15 kb 3' UTR (red arrow). **(C)** *pros*^{long} RNA is detected by UTR-long probe that targets a unique region of the 15 kb 3' UTR and is only present in neurons (blue dotted line region). **(D)** *pros* intron B probe that only recognises the nascent transcripts of the *pros*^{long} isoform is detected exclusively in neurons (blue dotted line region).

Figure 3: *pros*^{long} isoform is required for the up-regulation of Pros protein in larval neurons

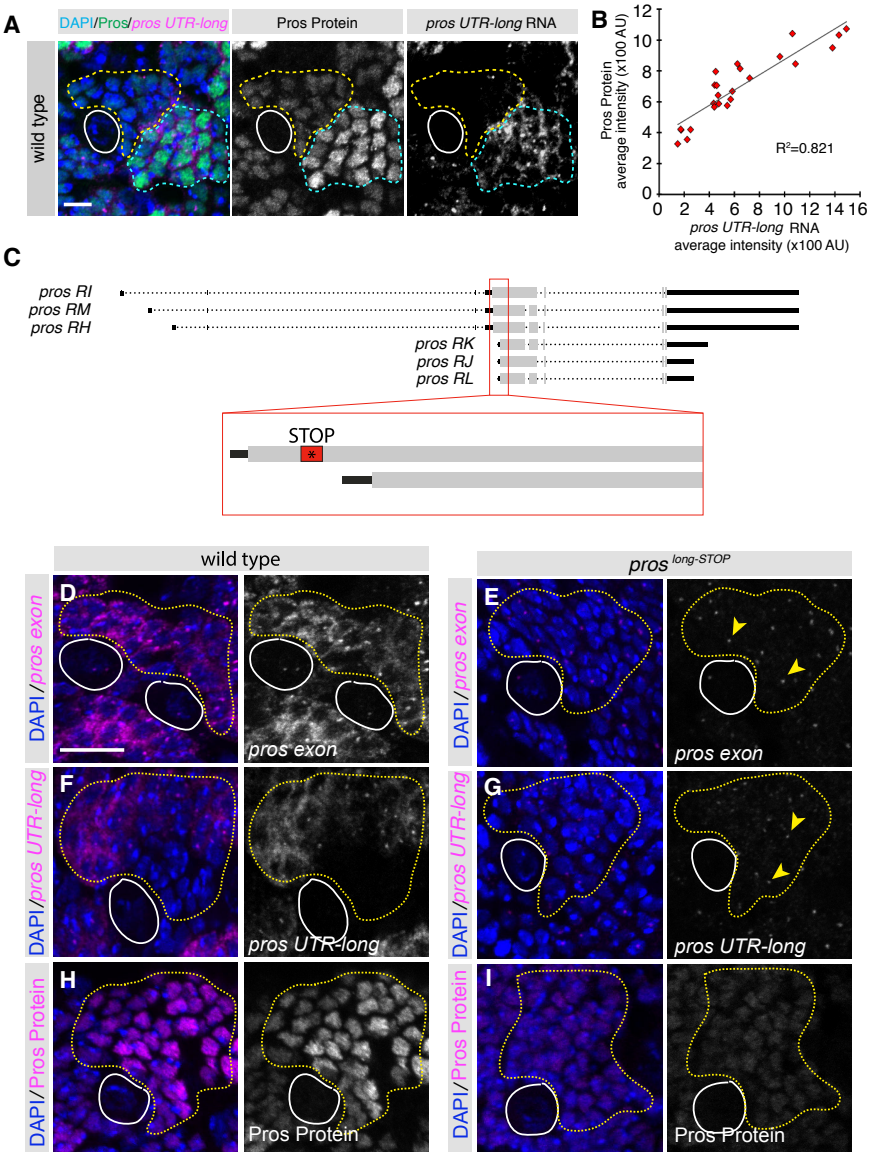

(A) Co-staining of Pros immunofluorescence with *pros* smFISH with UTR-long probe specific to *pros*^{long} isoform, show Pros protein expression level is increased where there is expression of the more stable *pros* transcript isoform with extended 15 kb 3' UTR. **(B)** Pros protein expression level is positively correlated with the expression of *pros*^{long} isoform. **(C)** Schematic of *pros*$^{long\text{-}STOP}$ mutant. A point mutation resulting in the formation of a stop codon is introduced downstream of the transcription start site (TSS) of the *pros*^{long} isoform but upstream of the *pros*^{short} isoform. This will induce degradation of the *pros*^{long} isoform transcripts via the NMD pathway. **(D-G)** RNA FISH confirming the successful elimination of the *pros*^{long} transcripts. Only transcription foci but not cytoplasmic mRNA, were detected using UTR-long probe that is specific to the *pros*^{long} isoform in the *pros*$^{long\text{-}STOP}$ mutant. Most cytoplasmic *pros*$^{long\text{-}STOP}$ transcripts are degraded by the NMD pathway following transcription. **(H-I)** Pros protein level is significantly reduced in *pros*$^{long\text{-}STOP}$ mutant and the neuron specific Pros up-regulation is abolished.

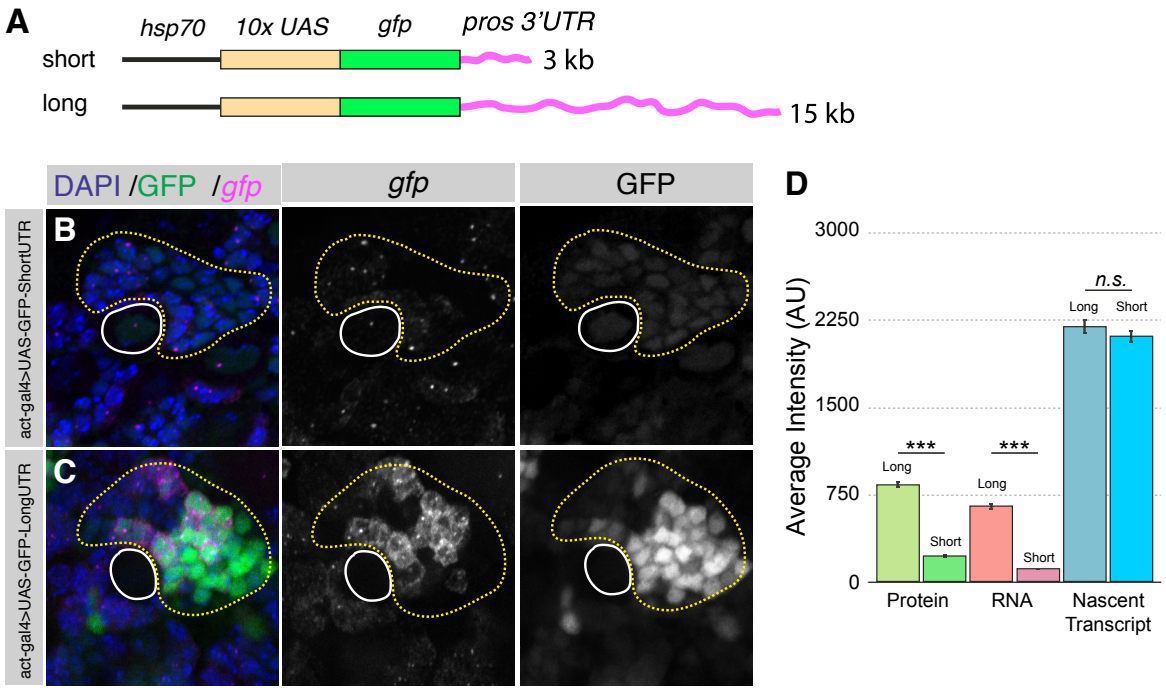

Figure 4: 15 kb 3' UTR of *pros*^{long} isoform is sufficient to increase transcript stability

(A) GFP transgene with 10x UAS was constructed to either contain the 3 kb 3' UTR of the *pros*^{short} isoform or the 15 kb 3' UTR of the *pros*^{long} isoform and the transgene was expressed using the UAS/GAL4 system. **(B-C)** Both RNA **(B)** and protein level **(C)** is significantly lower for transgene with the 3 kb *pros* 3' UTR, whereas the level of nascent transcript is not significantly different. This shows the long *pros* 3' UTR is sufficient to increase transcript stability. **(D)** Quantitative analysis of protein, RNA and nascent transcript level of the long and short *gfp* transgene.

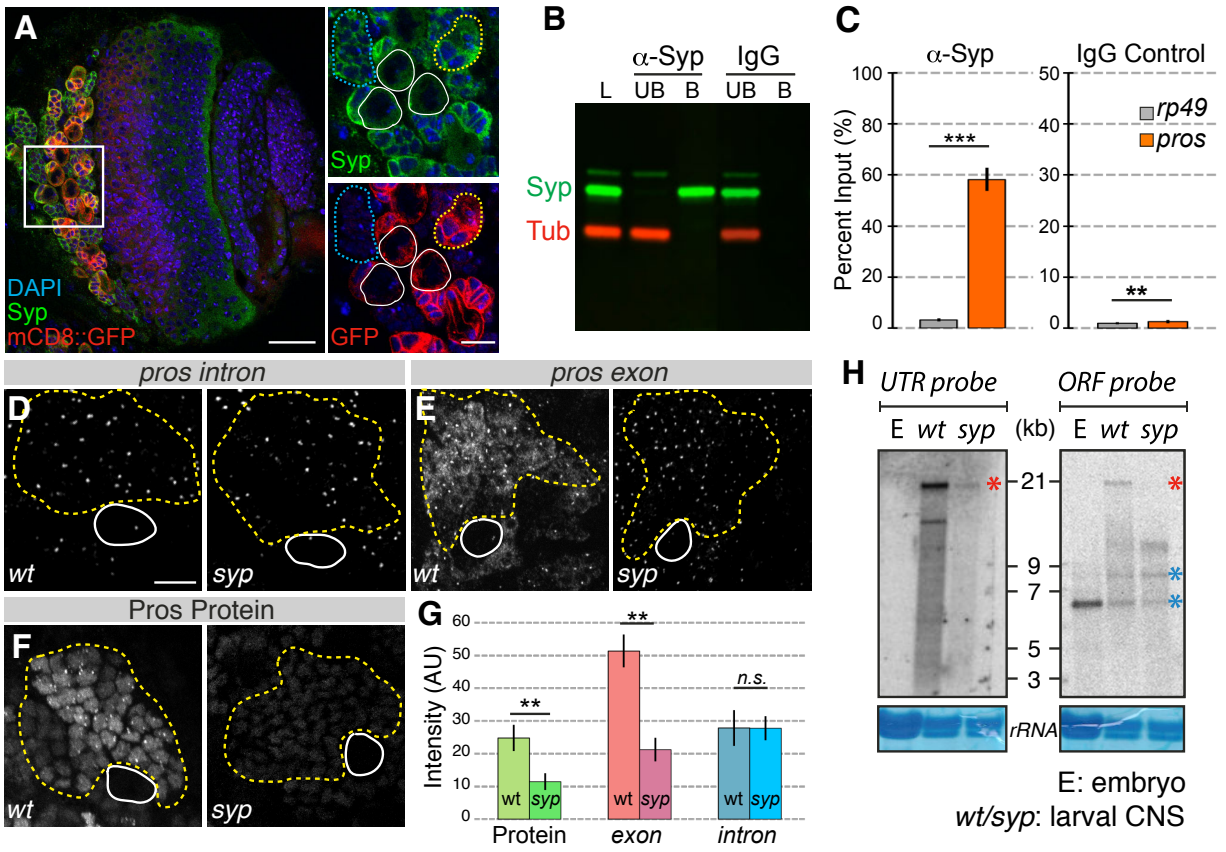

Figure 5: Syncrip selectively stabilises the *pros*^{long} isoforms in neurons

(A) Syncrip (Syp) protein is enriched in NB and progeny in 3rd instar larvae. Scale bars: 20 μm and 10 μm **(B)** Western blot confirming Syp can be immunoprecipitated (IP) selectively and efficiently. α-Tubulin (Tub) was used as negative control. **(C)** *pros* RNA is enriched by Syp IP but not by IgG control beads. Negative control, ribosomal *rp49* (*n*=7). **(D)** Syp does not affect primary transcription levels of *pros*, **(E)** but cytoplasmic *pros* *m*RNA levels are significantly reduced in *syp* mutants. **(F)** Up-regulation of Pros protein in neurons is abolished in the absence of Syp. **(G)** Quantitation of change in *pros* nascent transcripts, total mRNA and protein levels in *syp* mutant. **(H)** Northern blot showing the selective loss of *pros*^{long} isoforms in *syp* mutants. The intensity of the 6.5 kb and 9 kb bands are similar between wild type and *syp* mutants (blue asterisks) whereas the 21 kb band is significantly reduced in *syp* mutants (red asterisk).

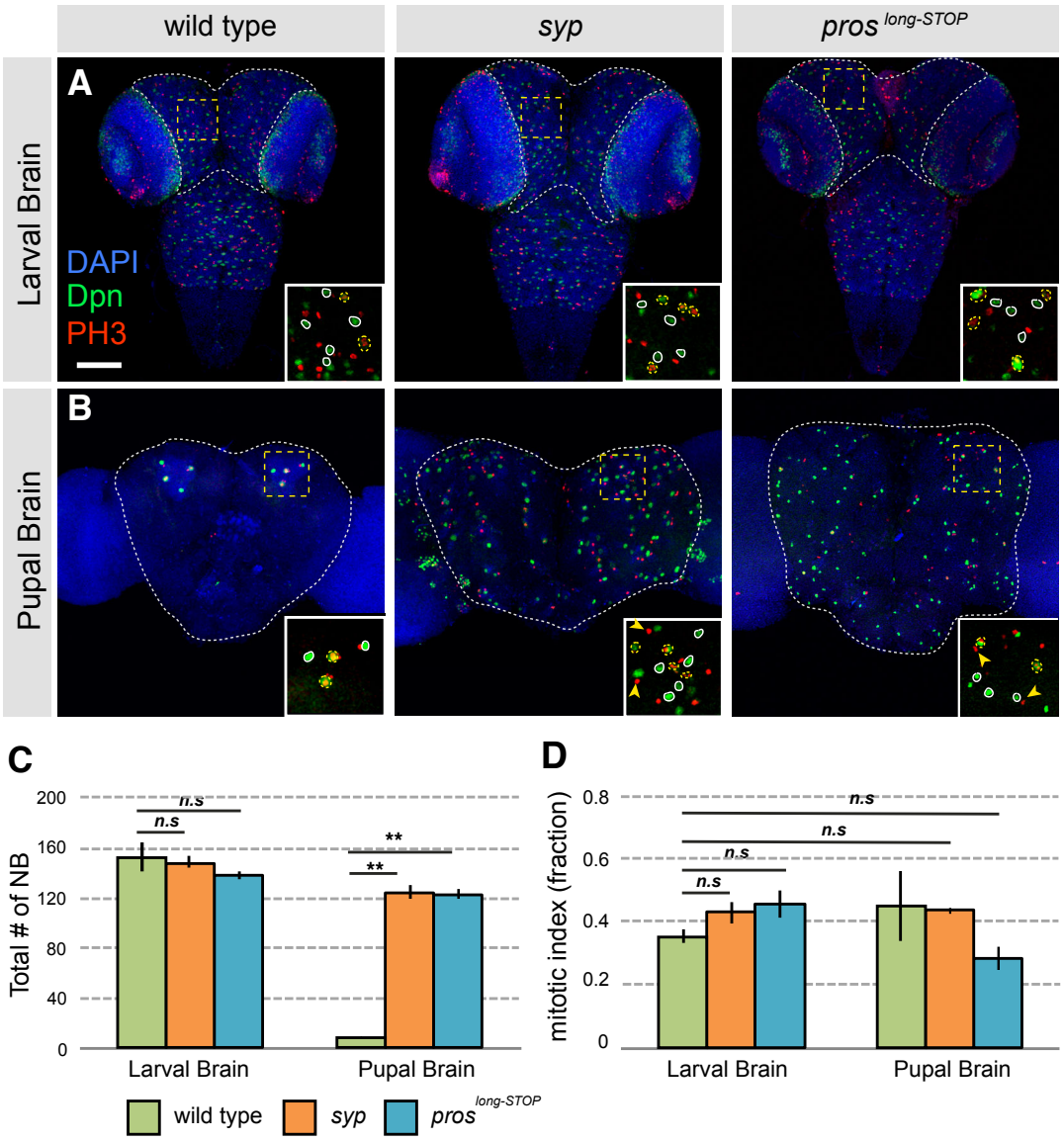

Figure 6: *pros*^{long} is not required to maintain larval neurons in differentiated states but is essential for pupal NBs to exit division

(A-B) NBs and dividing cells in the central brain region (grey dotted line) in larval **(A)** (72 hours after larval hatching) and pupal **(B)** (48 hours after pupal formation) brains, are labeled for Deadpan (green) and phospho-histone 3 (red), respectively. Inserts show clusters of dividing (yellow dotted outline) and non-dividing (white outline) NBs. Note Deadpan becomes faint and cytoplasmic in dividing NBs. PH3^{+}Dpn^{-} cells were also detected in close proximity to NBs, these cells are likely to be dividing GMCs produced from NB asymmetric division (yellow arrows). Scale bar: 50 μm. **(C-D)** Total NB number **(C)** is significantly increased in *syp* and *pros*$^{long\text{-}STOP}$ pupae, while mitotic index **(D)** is unchanged from the wild type larva, as NBs failed to terminate proliferation.

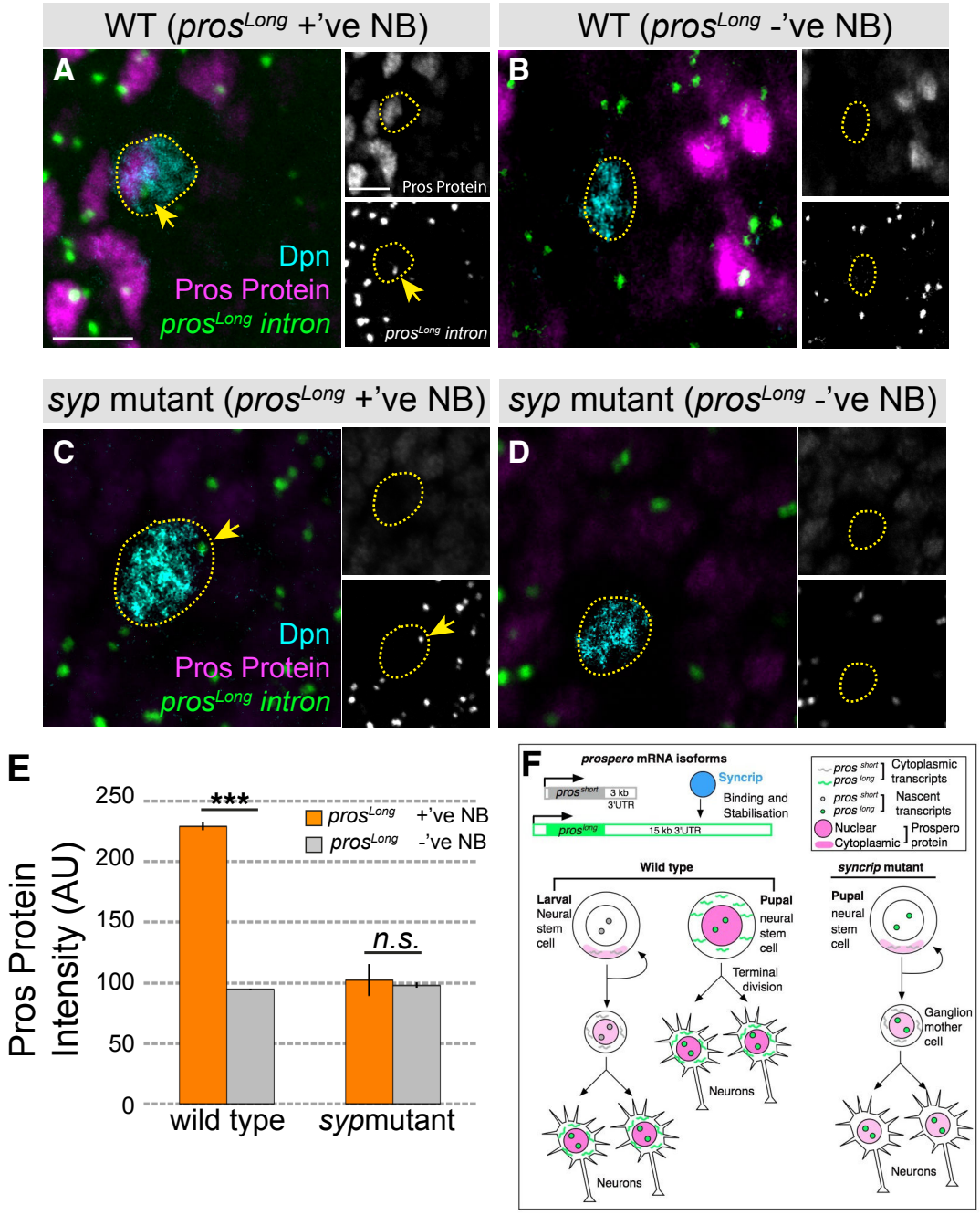

Figure 7: Transient up-regulation of Pros in terminal pupal NBs is achieved through Syp-dependent stabilisation of *pros^long^*

(A-B) Up-regulation of Pros protein in pupal NBs correlates with the activation of *pros^long^* transcription (yellow arrow) in wild type pupal brain. **(C-D)** *pros^long^* transcription (intron B probe, see Figure 2A) is not affected in *syp* mutant but nuclear Pros fails to up-regulate. **(E)** Quantification of Pros protein level in pupal NBs before and after *pros^long^* transcription activation; *n*=5 for Pros immunofluorescent quantification. **(F)** Graphical summary of *pros^long^* stabilisation by Syp triggering pupal NB exit from proliferation.

STAR★METHODS

KEY RESOURCES TABLE

REAGENT OR RESOURCE	SOURCE	IDENTIFIER
Antibodies		
Guinea pig anti-Syncrip	I.Davis Lab (McDermott *et al.* 2012)	N/A
Mouse anti-Prospero	Abcam	ab196361
Guinea pig anti-Asense	Gift from JA Knoblich	N/A
Rat anti-Deadpan	Abcam	ab195173
Mouse anti-αTubulin	Abcam	ab7291
Rabbit anti-Actin	Abcam	ab8227
Rabbit anti-histone	Abcam	ab18521
Rabbit anti-Histone H3 (phospho S28)	Abcam	ab10543
Donkey anti-Guinea pig IRDye®800CW	Licor	P/N 925-32411
Donkey anti-Guinea Mouse IRDye®680RD	Licor	P/N 925-68072
Goat anti-Mouse Alexa Fluor 488	ThermoFischer	A-11001
Goat anti-Guinea Pig Alexa Fluor 647	ThermoFischer	A-21450
Goat anti-Rabbit Alexa Fluor 594	ThermoFischer	R37117
Goat anti-Mouse Alexa Fluor 647	ThermoFischer	A-32728
Bacterial Strain		
Stellar™competent cells	Takara Clontech	PT-50552
One Shot® competent cells	ThermoFischer	C404010
Chemicals, Peptides, and Recombinant Proteins		
Dextran Sulfate 50% Solution	Sigma-Aldrich	S4030
VECTASHIELD Antifade Mounting Medium	VECTOR Laboratories	H-1000
Formaldehyde, 16%, methanol free, Ultra Pure	Polysciences, Inc.	18814-20
Liberase™ Research Grade	Roche	5401020001

REAGENT OR RESOURCE	SOURCE	IDENTIFIER
Critical Commercial Assays		
QIAPrep Spin Miniprep Kit	Qiagen	27106
Illustra™ RNAspin Mini Isolation Kit	GE Healthcare	45-001-163
Prime-a-Gene Labelling System	Promega	U1100
SYBR Green qPCR Master Mix	ThermoFischer	K0221
PCR Master Mix HotShot Diamond	Clent Life Science	HS002
LC Green Plus+	BioFire	BCHM-ASY-0005
Protein A magnetic beads	Abcam	ab214286
NEBNext® Poly(A) mRNA Magnetic Isolation Module	New England Bio Labs	E7490L
Ion Total RNA-Seq Kit v2	ThermoFischer	4475936
Ion PI IC 200 Kit	ThermoFischer	4488377
Taq DNA Polymerase	New England Bio Labs	M0273S
TOPO® TA Cloning Kit for Sequencing	ThermoFischer	K4575J10
In-fusion® HD cloning Kit	Takara Clontech	638906
Deposited Data		
RNA sequencing data of larval brains from wild type and *syncrip* mutant	Gene Expression Omnibus (GEO)	Acquisition in progress
Experimental Models: Organisms/Strains		
Drosophila: Oregon-R	Bloomington	2376
Drosophila: w[11180]; Df(3R)BSC124/TM6B	Bloomington	9289
Drosophila: P{GMR22F11-GAL4}attP2	Bloomington	48995
Drosophila: pros$^{Long\text{-}STOP}$	This Study	N/A
Drosophila: 10xUAS-hsp70-mCD8::GFP-Long3'UTR	This Study	N/A
Drosophila: 10xUAS-hsp70-mCD8::GFP-Short3'UTR	This Study	N/A
Drosophila: ase-GAL4	Gift from JA Knoblich	N/A
Drosophila: UAS-mCD8::GFP	Bloomington	5137
Oligonucleotides		

REAGENT OR RESOURCE	SOURCE	IDENTIFIER
Primers for Northern blot	This Study	see Table S1
Primers for Poly(A) Site Mapping	This Study	see Table S2
Primers for RT-qPCR	This Study	see Table S3
Stellaris® DNA probe set	BioResearch Technologies	see Table S4
Recombinant DNA		
pJFRC-10xUAS-IVS-GFP-WPRE	Addgene (Pfeiffer *at al.* 2010)	26223
P[acman] BAC CH322-77I07	BAC Resource	CH322-77I7
attB-P[acman]-Cm^{R}-BW	BACPAC Resources	N/A
Drosophila: pros$^{Long-STOP}$	This Study	N/A
Drosophila: 10xUAS-hsp70-mCD8::GFP-Long3'UTR	This Study	N/A
Software and Algorithms		
Fiji ImageJ 1.45r	Schindelin *et al.* 2012	*http://imagej.nih.gov/ij*
Bitplane: Imaris	*Bitplane*	*http://www.bitplane.com/*
Microsoft Excel	*Microsoft Cooperation*	150722
Image Studio	*LI-COR*	*https://www.licor.com/bio/products/software/image_studio*
TopHat Aligner v2.0.13	*Kim et al. 2013*	*https://ccb.jhu.edu/software/tophat*
DeSeq 2	Bioconductor (Love *et al.* 2014)	*https://www.licor.com/bio/products/software/image_studio*
SnapGene	*SnapGene*	*http://www.snapgene.com/*

CONTACT FOR REAGENT AND RESOURCE SHARING

For further information and access to any reagents and fly strains used in this manuscript, please contact co-corresponding author Ilan Davis (ilan.davis@bioch.ox.ac.uk).

EXPERIMENTAL MODEL AND SUBJECT DETAILS

Fly Genetics

All strains were raised on standard cornmeal-agar medium at 25 ℃. Oregon-R (*OrR*) was used as the wild type strain. *syncrip* mutants were *w[11180]; Df(3R)BSC124/TM6B* (Bloomington Deletion Project, Bloomington Stock 9289). Details on the generation of *UAS-GFP-pros-3'UTR* transgenic flies (10x*UAS-mCD8::GFP-Long3'UTR;* 10x*UAS-mCD8::GFP-Short3'UTR*) can be found in Method Details under the subheading "*prospero* 3' UTR transgene experiments". $pros^{long\text{-}STOP}$ mutants were generated using CRISPR technology, details are described in section "$pros^{long\text{-}STOP}$ mutant generation using CRISPR" (Method Details). Other stocks used in the study include: *UAS-mCD8::GFP* (Bloomington Stock 5137); type I neuroblast driver *ase-GAL4* was a generous gift from J.A. Knoblich lab (Zhu *et al.,* 2006); type II neuroblast driver P{GMR22F11-GAL4}attP2 (Bloomington Stock 48995).

METHOD DETAILS

prospero 3' UTR transgene experiments

prospero (pros) 3' UTR GFP transgene constructs containing full length *pros* 3' UTR were generated by inserting the *10xUAS::hsp70::eGFP* (*Drosophila* codon optimised) fragment (PCR from plasmid *pJFRC-10xUAS-IVS-GFP-WPRE*; Addgene) upstream of the *pros* 3' UTR from the BAC plasmid (*CH322-77I07*; P[acman] Resources; (*Venken et al., 2006*). For the GFP transgene construct containing the first 3 kb of *pros* 3' UTR, the 3' UTR fragment was first PCR'd from BAC (*CH322-77I07*) and inserted along with the *10xUAS::hsp70::eGFP* fragment into the *attB-P[acman]-*Cm^R*-BW* vector [P[acman] Resources; (*Venken et al., 2006*)].

Ligations of multiple inserts were accomplished using the In-Fusion cloning kit (Clonetech). Total reaction mixture varied between 10 to 20 µl. Reaction mixture was incubated for 15 min at 50 ˚C and was immediately used for transformation into Stellar™ competent cells (Clonetech). Plasmid DNA was extracted using the QIAprep Spin Miniprep Kit (Qiagen) following the manufacturer's instructions.

For generating BAC insertion transgenic flies, embryo injection was done by GenetiVision (Houston, Texas, USA). For each genotype, between 400-600 embryos were injected and screened.

pros$^{long\text{-}STOP}$ mutant generation using CRISPR

sgRNA construct design and validation was performed by Dr. Andrew Bassett - Genome Engineering Oxford (GEO). sgRNA (CCTCACAAGTCAACGGCGACGGC) targeting coding region that is unique to the *pros*^{Long} isoform was injected into 400 *vasa-cas9* embryos (Bloomington Stock: BL55821) as previously described (*Bassett and Liu, 2014*). Surviving embryos were crossed to a double-balancer stock TM3/TM6 and progeny were screened using high-resolution melt analysis (HRMA). Candidate mutant PCR products from the HRMA analysis were sequenced to confirm the introduction and location of the STOP codon.

Antibodies

The following primary antibodies were used: guinea pig anti-Syp (raised in the Davis lab as described in McDermott *et al.*, 2012 (*39*); western blot (WB) 1:2000; immuno-fluorescence (IF) 1:100; IP 1mg/ml); mouse anti-Pros (Abcam, IF 1:100); guinea pig anti-asense (IF 1:200; gift from J.A. Knoblich lab); rat anti-Deadpan (Abcam, IF 1:100); mouse anti-αTub (Abcam, WB 1:2000); rabbit anti-actin (WB 1:50); rabbit anti-histone (WB 1:200); rabbit anti-histone H3 (phospho S10) (Abcam IF 1:500). For quantitative western blot, the following secondary antibodies were used: donkey anti-guinea pig IRDye®800CW (1:2500); donkey anti-mouse IRDye®680CW (1:2500) (Chromotek). For IF, the following secondary antibodies were used at 1:250 dilution: Goat anti-Mouse Alexa Fluor 488; Goat anti-Guinea pig Alexa Fluor 647; Goat anti-Rabbit Alexa Fluor 594.

RNA extraction

RNA extraction was performed using the RNAspin RNA Isolation kit (GE Healthcare). Modified manufacture instructions for RNA purification form cultured cells were followed with modifications to accommodate *Drosophila* samples. 3rd instar larval brains were homogenised in 30 µl of RA1 buffer including 2 µl 40 U/µl RNAse inhibitor (RNAsin® Plus RNase Inhibitor (Promega)). Additional RA1 buffer was added to lysate after homogenisation to make up a total volume of 350 µl. An equal volume of 70% ethanol was added to the lysate and pipetted up down several times to allow good mixing. The lysate/ethanol solution was loaded onto the RNAspin Mini column and centrifuged for 30 s at 8,000 x *g*. Following centrifugation, the flow

through was discarded and the spin column was transferred to a fresh 1.5 ml collecting eppendorf tube. 350 µl of membrane desalting buffer (MDB) was added to the column followed by 1 min centrifugation at 11,000 x *g*. In column DNA digestion was done by directly adding a 100 µl of DNase digestion solution (10 µl reconstituted DNAse I; 90 µl DNAse reaction buffer) to the RNAspin column and allowed to incubate at RT for 15 min. The column was subsequently washed with 200 µl RA2, 600 µl RA3 and 250 µl of RA3 buffer, each wash followed by centrifugation at 11, 000 x *g* for 1 min. After final wash, 40 µl of nuclease free H_2O was applied to the column to elute the bound RNA and elute was collected by centrifugation at 11,000 x *g* for 1 min. To increase yield, elute was re-applied to the column and eluted a second time. Concentration of RNA was measured on either Nano-drop or RNA Fluorometer (Qubit). Extracted RNA could then be flash frozen with liquid nitrogen and stored at -80 ˚C or directly processed for cDNA library synthesis or Northern blot.

Western blot

NuPage Novex 4-12% Bis-Tris gels (Invitrogen) were used for all SDS-PAGE experiments. Following SDS-PAGE, proteins were transferred to nitrocellulose membrane using the XCell II™ Blot Module (Invitrogen) following manufacturer's protocol. Protein bands were visualised with the quantitative infrared imaging system (LI-COR Odyssey, LI-COR Biosciences; Lincoln, NE). Intensity of protein bands was quantified using the LI-COR software.

Northern blot

5 µl of purified RNA samples was mixed with 3.5 µl 37% formaldehyde and 10 µl 100% formamide, 2 µl supplemented 10x MOPS buffer (400 mM MOPS buffer, 100 mM NaOAc , 10 mM Na_2EDTA). Sample mixture was incubated at 55 ˚C for 15 min and 4 µl of loading dye (1 mM EDTA, 0.25% BromoPhenolBlue, 50% Glycerol) was added and ran on an 1.5% agarose gel at 120 V in 1x MOPS buffer. ssRNA ladder (NEB) was used as size marker for all Northern experiments.

RNA was transferred to pre-wet Nylon membrane (Hybond-N, Amersham). Blotted RNA was cross linked to the membrane with either a UV crosslinker or by baking at 80 ˚C for >1 hr.

The membrane was hybridised in hybridisation buffer (0.4 M Na_2HPO_4, 6% SDS and 1 mM EDTA) for 1 hr at 57 ˚C with RNA probes prepared using the Prime-a-Gene kit (Promega) (For list of primers used to generate RNA probes, see Table S1), washed twice with wash buffer 1 (40 mM Na_2HPO_4, 5% SDS and 1 mM EDTA) and twice with with wash buffer 2 (40 mM

Na_2HPO_4, 5% SDS and 1 mM EDTA). RNA was detected overnight in phosphorImager (Molecular Dynamics).

Real Time Quantitative PCR (RT-qPCR)

RT-qPCR was performed using a real time PCR detection system (CFX96 Touch™ Real-Time PCR Detection System (BioRad)) and in 25 µl consisted of : 12.5 µl 2x SYBRGreen Mastermix (ThermoFisher), 0.75 µl of gene specific primer (10 µM stock, forward and reverse), 4 µl of cDNA and 7 µl of nuclease free water. Cycle threshold (C(T)) value was calculated by the BioRad CFX software using a second differential maximum method. Each reaction was performed in duplicate and the average C(T) value was used. Relative mRNA levels were determined using the equation mean fold change $=2^{-\delta\delta C(T)}$ method described by Livak and Schmittgen (2001) (*40*). In brief, the C(T) values of the mRNA level were normalised to the C(T) values of a reference gene in the same sample. This represents the relative fold change of the mRNA in comparison to control. Percent input method was used to assess immunoprecipitation efficiency. Standard curve of percent input v.s. C(T) value was plotted and equation of the standard curve was used to calculate percent input of the immunoprecipitation samples.

High Resolution Melt Analysis (HRMA) PCR

HRMA PCR was used to screen CRISPR induced mutants (*Bassett and Liu, 2014*). Genomic DNA was extracted from mutant flies and PCR was performed to amplify a 100-200 bp products spanning the targeted site. PCR reactions were performed in a 10 µl reaction mixture consisted of: 1 µl of genomic DNA, 5 µl of 2x Hotshot Diamond PCR mix (Clent Life Science), 0.2 µl of gene specific forward and reverse primer each (10 µM stock), 1 µl of 10x LC Green and 2.6 µl of nuclease free water. Product was amplified using the following cycle: 95 ˚C for 5 min, 45 cycles of [(95 ˚C for 10s, 55-65 ˚C for 30 s (exact temperature depends on the Tm of the primer set) and 72 ˚C for 30s], 95 ˚C for 30 s and 25 ˚C for 30 s. PCR product was then subjected to HRM (range 70-98 ˚C, equilibrate at 67 ˚C) followed by HRMA using the RotorGeneQ software. Melt curve fluorescence was normalised to the region of the curve before and after the melt.

Immunoprecipitation

Guinea pig anti-Syp antibody and IgG antibody were cross-linked to ProteinA magnetic beads (Abcam) following manufacturer's protocol. For each replicate, 90 third instar larval brains dissected in Schneider medium were homogenised in immunoprecipitation (IP) buffer (50 mM Tris-HCl pH 8.0, 150 mM NaCl, 0.5% NP-40, 10% glycerol, 1 mini tablet of Complete EDTA-free

protease inhibitor and 2 µl RNAse inhibitor (RNAsin® Plus RNase Inhibitor (Promega)) and topped up to 100 µl in IP buffer. For each reaction, 20 µl of lysate was taken as a 50% input sample which was taken directly to RNA extraction. 40 µl of lysate was incubated with 25 µl of each antibody cross-linked beads over night at 4 ˚C on rotator wheel. For each reaction, 100 µl of lysate was incubated with 20 µl of 50% bead slurry over night at 4 ˚C on rotator wheel. Next day, supernatant was transferred to fresh tubes and beads were washed 5 times for 5 min each with 200 µl cold IP buffer at 4 ˚C. After final wash, beads were resuspended in 40 µl extraction buffer (50 mM Tris-HCl pH 8.0, 10 mM EDTA and 1.3% SDS, 1:100 RNAsin) and incubated at 65 ˚C, 1000 rpm for 30 min on thermomixer. The elution step was repeated and the supernatant were pooled. RNA was then extracted from the IP eluates and the input sample and used for cDNA library synthesis.

RNA Sequencing

Three biological replicates (*n*=3), each replicate consists of a pool of 100 larval brains. Following RNA extraction, mRNA was enriched using NEB Next® Poly(A) mRNA Magnetic Isolation Module (NEB). Briefly, extracted RNA sample was mixed with Oligo $d(T)_{25}$ beads and heated to 65 ˚C for 5 min followed by incubation at 4 ˚C for 1 hr to allow binding. Following incubation, the beads were washed 5 times for 5 min each at 4 ˚C and RNA was eluted by heating the beads at 80 ˚C for 5 min. Poly(A) enriched RNA was then used for library production using the Ion Total RNA-Seq Kit v2 for Whole Transcriptome Libraries (Life Technologies). Following quality control steps, adaptors were hybridised to the RNA fragments and RT reaction was performed followed by cDNA amplification with Ion Xpress RNA Barcode primers. Prior to sequencing, quality of cDNA libraries were assessed using Agilent High Sensitivity DNA Kit with the Agilent 2100 Bioanalyser. Libraries were pooled to a total concentration of 100 pM, with three samples multiplexed per chip. Sequencing was performed on an Ion Proton Sequencer, using the Ion PI IC 200 Kit (Life Technologies). Ion PI chips were prepared following manufacturer's instructions and loaded using the Ion Chef System.

Poly(A)-site mapping

Poly(A)-site mapping was carried out using the method described in (*Davis and Ish-Horowicz, 1991*). In short, RNA was extracted from wild type larval brains and cDNA library was generated using a poly(T) primer containing a 5'G-C rich region and a NotI site. PCR reactions were subsequently carried out using the same poly(T) primer and a forward gene specific primer. The cDNA was purified using a standard PCR program except that instead of high fidelity Phusion DNA polymerase, 0.125 U Taq DNA polymerase (NEB) was used in a 25 µl volume (for

complete list of primers see Table S2). To optimise PCR, magnesium titration between 1 to 3 mM in 0.5 mM increments was tested. To increase the specificity of the PCR, nested PCR was performed using the product from the first PCR reaction. Product from nested PCR reaction was resolved on a 2.5% agarose gel and bands were extracted using the QIAquick Gel Extraction Kit (Qiagen) following manufacture's instructions. Extracted DNA product was cloned into a TOPO® vector using a TA cloning kit (Invitrogen). Single colonies was selected and cultured in LB medium containing the appropriate antibiotics. Plasmid DNA was extracted using QIAprep Spin Miniprep kit (Qiagen) and sequenced by Sanger Sequencing (Source BioScience).

Cytoplasmic and Nuclear Fractionation of Larval Brains

30 dissected larval brains were dissociated to single cells by first incubating in 1 mg/ml liberase (mixture of collegenase I and II; Roche) for 10 min at 37 ˚C followed by pipetting up and down 100 times. Following dissociation, cells were collected by centrifugation at 8,000 rpm for 10 min at 4 ˚C and supernatant were discarded. Dissociated cells were resuspended in 20 µl of hypotonic Buffer A (10 mM HEPES, 1.5 mM $MgCl_2$, 10 mM KCl, 0.5 mM DTT and 0.5 µl RNAse inhibitor, buffer prepared in ddH_2O) and incubated on ice for 5 min. Cells were then homogenised to release cytoplasmic content and nuclei were pelleted by centrifugation at 1,000 rpm for 5 min at 4 ˚C. Supernatant was removed to fresh tubes (Cytoplasmic fraction). The nuclei pellet was resuspended in 20 µl S1 sucrose buffer (0.25 mM sucrose, 10 mM $MgCl_2$ prepared in dH_2O containing protease inhibitor and RNAse inhibitor), layered over a 40 µl sucrose cushion (0.88 mM sucrose, 0.5 mM $MgCl_2$ prepared in dH_2O including protease and RNAse inhibitor and centrifuged at 2,800 rpm for 10 min at 4 ˚C. The supernatant was discarded and the clean nuclei pellet re-suspended in Buffer A. The fractionated cytoplasmic and nuclei fraction were used directly for subsequent protein analysis or RNA extraction.

Immunofluorescence

Third instar larval brains were dissected in Schneider's medium and fixed in 4% formaldehyde (FA) solution (4% FA in 0.3% PBTX) for 20 min at room temperature. Following incubation with primary and secondary antibody, samples were mounted in VECTASHIELD anti-fade mounting medium (Vector Laboratories).

Identification of larval neuroblast, ganglion mother cells and neurons

Neuroblasts (NBs) were identified based on their unique shape and location in the larval brain. Ganglion mother cells (GMCs), new born and differentiating neurons were distinguished from each other using a previously described method based on *asense(ase)-GAL4>mCD8::GFP*

fluorescence intensity levels, as GFP intensity decreases with GMC maturation and division (Neumuller *et al.,* 2011). This classification method using mCD8::GFP fluorescence intensity was validated by performing immunofluorescence (IF) using cell type-specific antibodies (NBs: Dpn^{+},Ase^{+}; GMCs: Dpn^{-},Ase^{+}; neurons: Dpn^{+},Ase^{+}).

RNA single molecule fluorescent *in situ* hybridisation (smFISH) for larval brains

Dissected 3rd instar larval brains were fixed in 4% paraformaldehyde (PFA) solution for 30 min at room temperature followed by 3 rinses in 0.3 % PBTX (PBS and 0.3% triton). Samples were washed 2 times for 20 minutes each in 0.3% PBTX at RT and incubated in pre-hybrdisation buffer (10% deionised formamide in prepared in 2x SSC) for 5 min at 37 ˚C. Hybridisation was performed by incubating samples overnight at 37 ˚C in the dark with gentle shaking in hybridisation buffer (10% deionised formamide, 5% dextran sulphate (sigma), 2x SSC) containing 250 nM gene specific fluorescently labeled Stellaris® DNA probe set (BioSearch Technologies). Following hybridisation, samples were rinsed 3 times in pre-hybridisation buffer and washed for a further 3 times, 30 min each time in pre-hybridisation buffer at 37 ˚C. DAPI was included during the second 30 min wash. A final two washes were performed using 2x SSC for 10 min each at room temperature and samples were mounted in VECTASHIELD anti-fade mounting medium (Vector Laboratories) and immediately imaged using point scanning confocal microscope. Samples were protected from light for all steps including hybridisation.

smFISH with immunofluorescence for larval brains

The protocol is identical to the smFISH protocol except for the following modifications. Before hybridisation, samples were blocked in blocking buffer (1% BSA in 0.3% PBTX) for 1 h at room temperature. Antibody at the appropriate dilution was included with the Stellaris® DNA probes during the over night hybridisation step. Counter-stain with secondary antibody was performed on the second day following hybridisation. After final wash, samples were mounted in VECTASHIELD anti-fade mounting medium (Vector Laboratories) and immediately imaged.

Image acquisition

Fixed imaging of larval brain was performed using an inverted Olympus FV1000 Laser Scanning Microsope with Becker and Hickel FLIM system and with an inverted Olympus FV1200 Laser Scanning Microscope with high sensitivity galium arsenide phosphide (GaAsP) detectors (Olympus). Images were acquired using x20 0.75 NA UPlanSApo, x 40 1.3 NA Oil UPlan FLN, x60 1.4 NA and x100 1.4 NA Oil UPlanSApo objective lenses. Laser units used were: solid state 405 and 488 laser, argon 488, 515, 568 and 633 laser.

Quantification and statistical analysis

Except for analysis of RNA sequencing data (see section "Bioinformatic analysis of RNA sequencing data"), all statistical analysis was performed using Microsoft Excel. For all bar graphs unless otherwise stated, data represents means ± standard error of the means (SEMs). Two tailed Student's t-test was used to compare different genotypes or cell types. Significance was classified as $p<0.05$.

Data analysis for Immunoprecipitation

For each of three biological replicates, a dilution series of the input sample was produced (10%, 2%, 0.5%. 0.01% of input). qPCR for each set of primers was performed on this series and the Cq values were plotted against log10 dilution to find the formula of the line. The Cq value of each pulldown sample (anti-Syp and anti-IgG) was inputted into this formula to calculate the % of input pulled down. For each set of primers, a two tailed Student's t-test was used to compare the % input pulldown in the test (anti-Syp) and control (anti-IgG) samples.

Bioinformatic analysis of RNA sequencing data

Base calling, read trimming and sample de-multiplexing was done using the standard Ion Torrent Suite. The reads were aligned to the *Drosophila* genome (ENSEMBL assembly BDGP5, downloaded 8 Jan 2015) using the TopHat aligner (v2.0.13) (*Kim et al. 2013*). To quantitate gene expression, uniquely aligned reads were assigned to the *Drosophila* exome (BDGP5) using htseq-count. Differential was assessed using negative binomial generalised linear models implemented in R/Bioconductor package DESeq2 (Love *et al.* 2014).

Image analysis for Immunofluorescence and smRNA FISH

The intensities of nascent transcript foci and cytoplasmic mRNA were analysed using method described in Zenklusen et al., 2008; Trcek et al., 2011. Briefly, for nascent transcript analysis, 3D image intron smFISH data set was first uploaded onto Imaris Image Analysis software (Imaris, Bitplane). Using the Gaussian mask based spot-detection algorithm (Imaris, Bitplas) which detects and quantifies the signal intensity of each spot, the intensity of individual nascent transcript foci was measured and the average intensity was calculated. For cytoplasmic RNA signal intensity and protein immunofluorescence intensity, the 3-dimensional exon smFISH image data was first reduced to a 2-dimensional image by maximum Z projection in FIJI (ImageJ 1.45r; M). Using membrane-tethered protein mCD8 staining which labels the nuclear and cytoplasmic membrane, a hand-drawn mask was created for the cytoplasmic region of the

cell of interest. The coordinates of the mask was saved and imported as region of interest (ROI) to FIJI and average intensity value for each pre-defined ROI was calculated using the “Measure” algorithm in FIJI.

Phenotype analysis for wild type, syncrip and *pros$^{long\text{-}STOP}$* larval and pupal mutant

Flies were allowed to lay for 2 h at 25 ˚C on apple juice plate. Hatched larvae were subsequently transferred to bottles containing standard fly food and larvae/pupae were removed at the appropriate time point for dissection. Two developmental stages were investigated: 72 h (3rd instar) after larval hatching (ALH) and 48 h after pupal formation (APF). Brains were dissected and fixed in 4% FA and subsequently stained with the neuroblast specific marker Deadpan (Dpn), and the mitotic marker phospho-histone 3 (PH3). Images of the ventral brain were acquired using Olympus point-scanning confocal microscope at 2 µm steps. Image analysis was completed using Imaris Image Analysis software (Imaris, Bitplane). For counting the total number of NBs, and cells that are both positive for Dpn and PH3, the “Point" tool in Fiji program was used. For each genotypes, three brains (*n=3*) was analysed.

DATA AND SOFTWARE AVAILABILITY

We are currently acquiring a Gene Expression Omnibus (GEO) accession number for the presented RNA sequencing data and will provide the number prior to publication.

SUPPLEMENTARY INFORMATION

Includes:

Figures S1: related to Figure 1
Figure S2: related to Figure 2
Figure S3: related to Figure 2
Figure S5: related to Figure 5
Figure S6: related to Figure 5
Table S1-3

Included as separate file:

Table S4 (as Word file): Sequence used to generate Stellaris® DNA probe set

Table S5 (as Excel file): RNA Sequencing results from wild type and *syncrip* mutant larval brains

SUPPLEMENTARY FIGURES

Figure S1: Using mCD8::GFP fluorescent intensity to indicate neuroblast progeny age

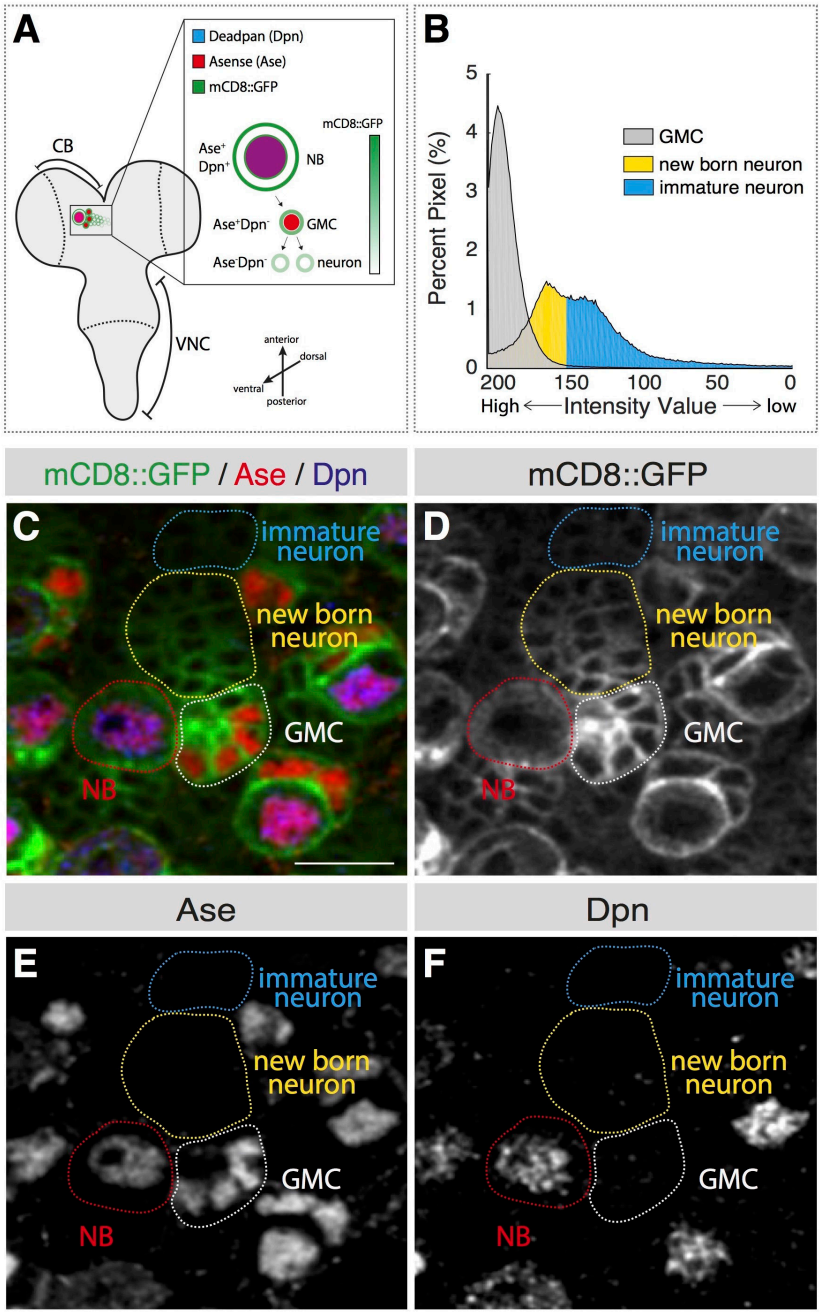

(A) Illustration of type I neuroblasts (NB) lineage in the 3rd instar larval brain labeled with *ase-gal4>UAS-mCD8::GFP*. NBs express both Ase and Dpn while Dpn expression is diminished in ganglion mother cells (GMCs) and early neurons. *ase-gal4>mCD8::GFP* intensity decreases with progeny age (Neumuller *et al.*, 2011). **(B)** GFP fluorescent intensity distribution in GMCs (grey) and neurons (new born - yellow, and differentiating - blue). **(C-F)** Confirmation of cell type identification using GFP intensity, using NB and progeny specific immunofluorescence (IF). NBs are identified based on their unique shape and location in the central brain (CB) and this is confirmed by Ase and Dpn IF (red dotted line region). Using GFP intensity thresholding, the majority of the identified GMCs are Ase^{+}, Dpn^{-} (white dotted line region) while early neurons are negative for both Ase and Dpn (yellow and blue dotted line region). Scale bar represents 10 μm.

Figure S2: Polyadenylation site (PAS) confirmation of prospero RNA using PCR

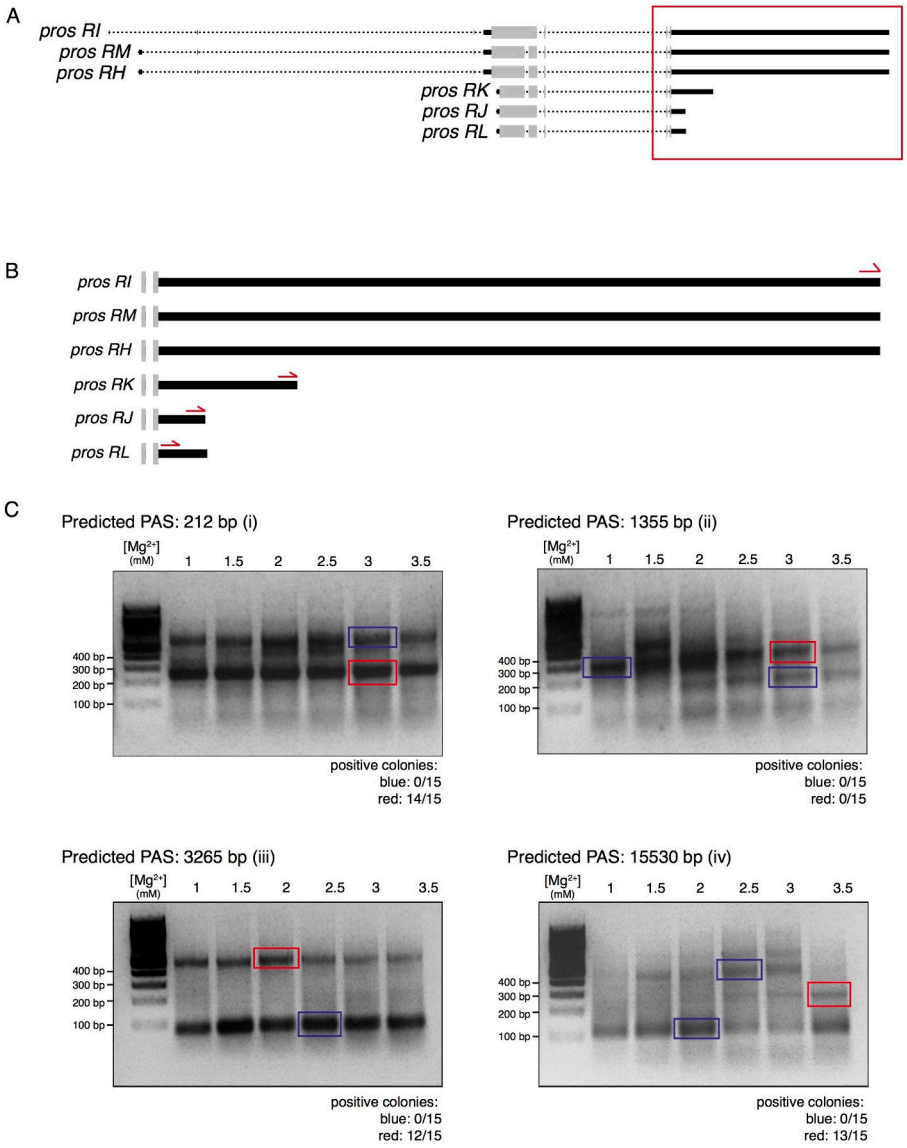

(A) 6 different *prospero* (*pros*) isoforms are annotated in FlyBase. *pros-RI*, *-RM* and *-RH* have a 15 kb 3' UTR, *pros RK* have a 3 kb 3' UTR and *pros-RJ* and *-RL* have a 1.2 kb 3' UTR. **(B)** Illustration showing PCR primers targeting the different PAS sites that were chosen to be tested. Four PASs were selected: 212 bp, 1.2 kb, 3 kb and 15 kb. The 212 bp was chosen as it is consistent with published Northern blot data of *pros* and the 1.2 kb, 3 kb and 15 kb sites were selected as they are the annotated *pros* PAS on FlyBase. **(C)** Agarose gel showing nested PCR product for each of the PAS. Red boxes are bands that occurred at the expected size, blue boxes are additional bands. Both red and blue box highlighted bands were gel extracted, amplified by TA cloning and 15 colonies for each band were selected and sequenced. The total number of selected colonies that were found to have sequences that mapped to the annotated PAS of *pros* are shown below each gel.

Figure S3: *pros*^{long} is only expressed in neurons and *pros*^{short} with 3 kb 3' UTR is the predominant isoform in NBs and GMCs

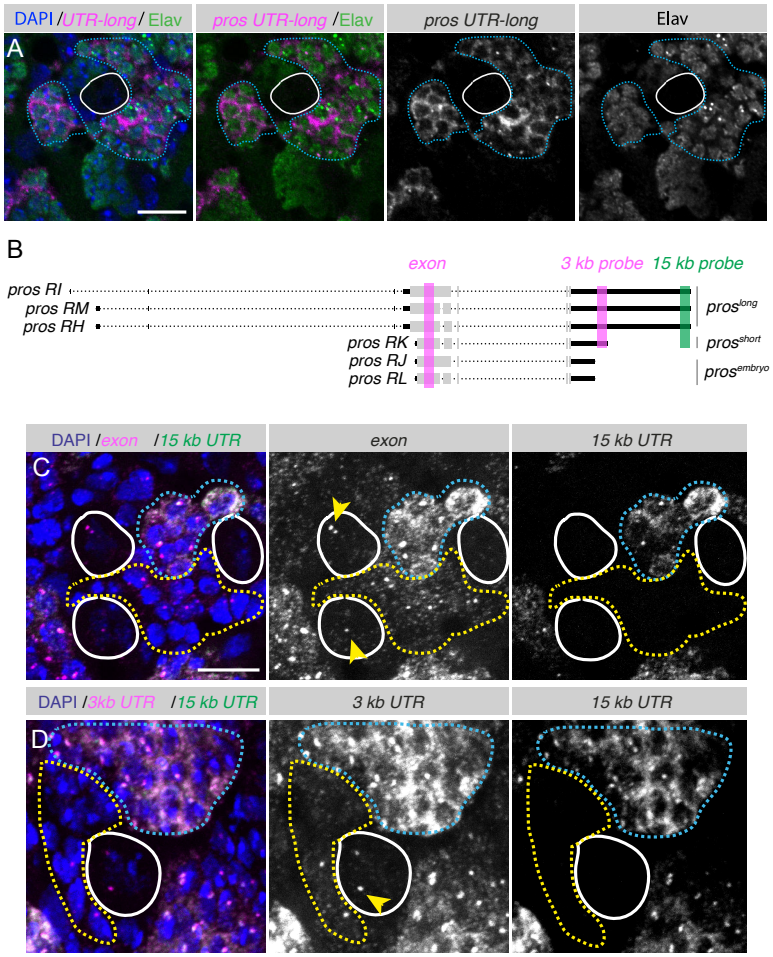

(A) Double labelling with smFISH probe that is specific to *pros*^{long} isoform (magenta) and neuron specific label Elav (green) show all cells that express *pros*^{long} isoform also express Elav (blue dotted region), demonstrating that *pros*^{long} is only expressed in neurons. **(B)** smFISH probe targeting exon (magenta); 3 kb 3' UTR (magenta) and 15 kb 3' UTR (green) region of the pros transcript. **(C - D)** High magnification images showing in NBs (white outlined region) and GMCs (yellow dotted region) signal intensity from *pros* exon and 3 kb 3' UTR probes are not significantly different suggesting the predominant *pros* transcripts in NBs and GMCs is the *pros*^{short} isoform. Note *pros* transcription foci in NBs could be clearly detected by both the exon and the 3' UTR probe (yellow arrow heads). The 15 kb 3' UTR probe was used to distinguish neurons from GMCs. Scale bar represents 10 µm.

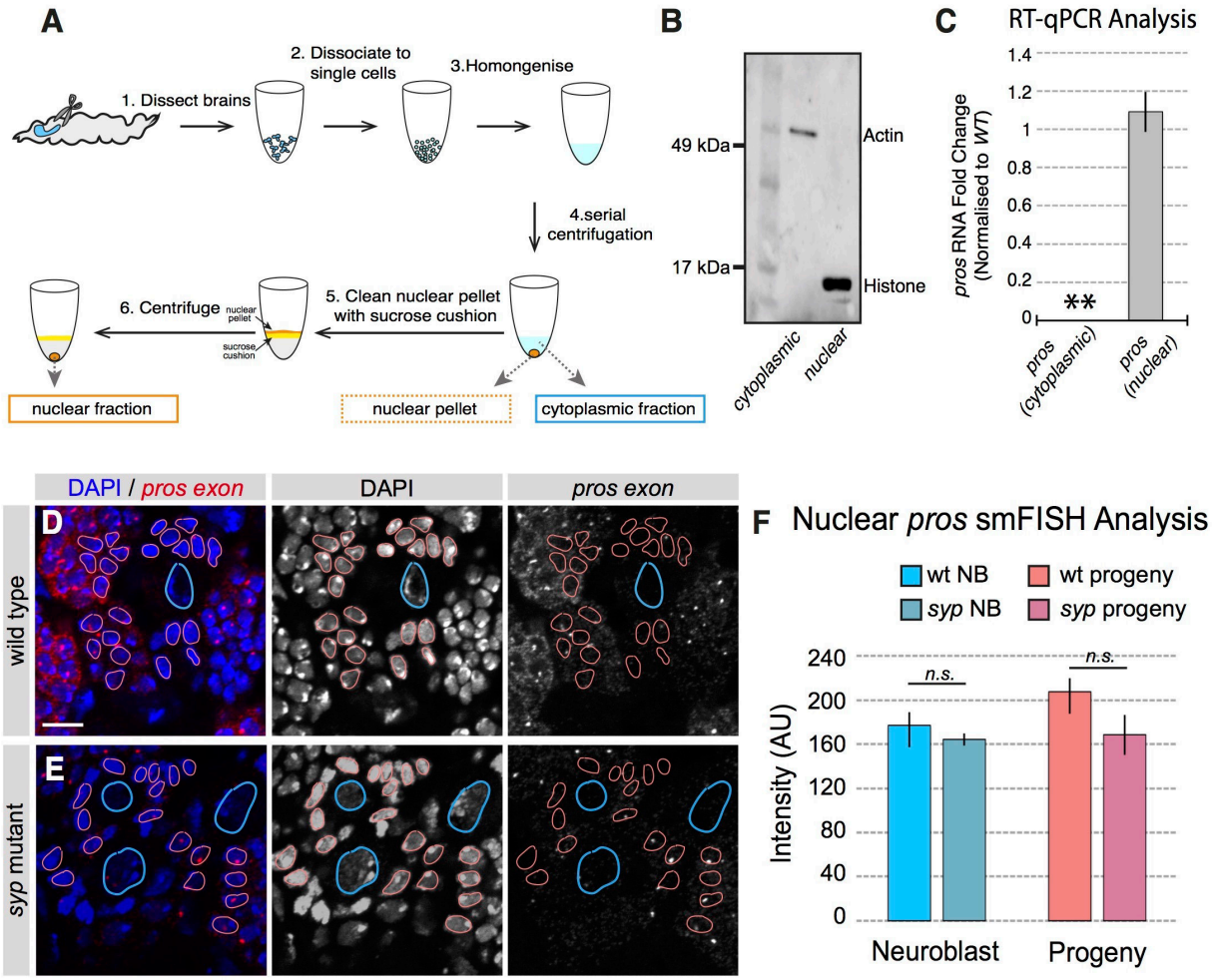

Figure S4: Biochemical confirmation of selective loss of cytoplasmic *pros* RNA in *syp* mutant

(A) Schematic of nuclear and cytoplasmic fractionation of larval brains (for details of the protocol, see Material and Methods) **(B)** Western blot blotted with anti-Actin (cytoplasmic) and anti-Histone (nuclear). WB showed minimal contamination between the cytoplasmic and nuclear fractions. **(C)** RT-qPCR analysis of *pros* RNA level in *syp* mutant in the cytoplasmic and nuclear fraction (normalised to wild type). Error bars represent SEM. ***pros* RNA in the cytoplasmic fraction from *syp* mutant failed to reach Cq threshold within 40 cycles. **(D-E)** *pros* mRNA is not retained in the nucleus in NBs (cyan outline regions) and NB progeny (magenta outline regions) in *syp* mutant. Scale bar represents 10 μm. **(F)** Quantification shows no significant difference between nuclear *pros* RNA level in wild type and *syp* mutant NB and NB progeny. *n=5* for NB; *n*=10 for progeny. *n.s. = not significant*.

Figure S5: *syp* mutants have specific loss of *pros*^{long} isoform and does not affect level of neuron specific *pros*^{long} transcription

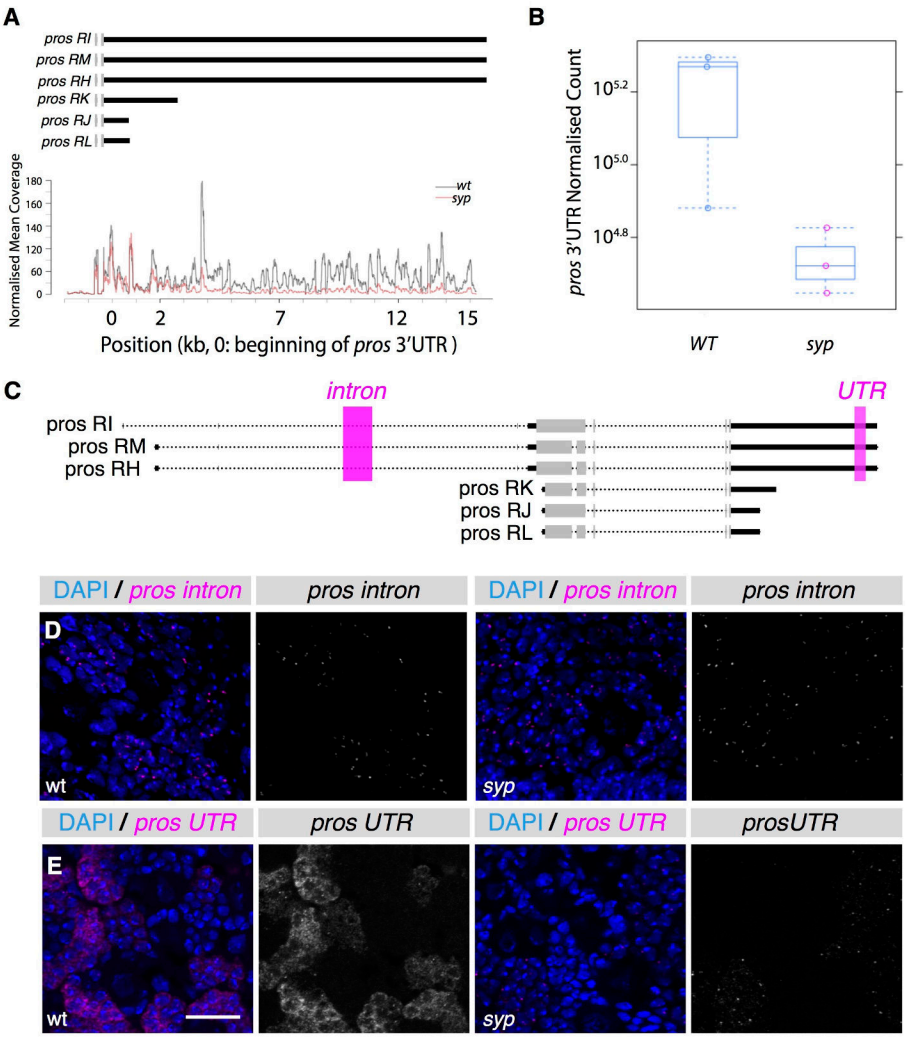

(A) RNA sequencing results showing selectively loss of *pros*^{long} isoform in *syp* mutants. Read coverage for the first 3 kb of *pros* 3' UTR was not different between wild type (wt) and *syncrip* (*syp*) mutant whereas the distal 12 kb of *pros* 3' UTR is reduced in *syp* mutants. **(B)** Quantitative analysis of total sequencing reads of *pros* 3' UTR in wild type and *syp* mutants. (****p<0.001*) **(C)** Diagram showing position of intron and UTR probe. **(D)** Syncrip does not affect transcription of the long isoform **(E)** Cytoplasmic transcript level of *pros*^{long} is significantly reduced in *syp* mutant suggesting Syp regulates *pros*^{long} transcript stability. scale bar represents 10 μm.

Name	Sequence (5' - 3')
ORF F1	AGAAGCGCAAGCTCTACCAG
ORF R1	GTCTTGGGTTTTAGGGGCGA
ORF F2	AAGAAACCCGGCATGGACTT
ORF R2	CGTCACCATCTCCGGTCAAA
UTR Long1 F	GACGATGGTGAACGCGAAAG
UTR Long1 R	TGTGGCTGTGTTCTTGTGGT
UTR Long2 F	ATTTCCCAATCGGCGTCCTT
UTR Long2 R	TTGCCTGTCGATTGCTCTGT
UTR Short1 F	TTGGATGGGAACACCGCTAC
UTR Short1 R	GTGCTCCAAAATCGGGCTTG
UTR Short2 F	CGCAGGCCAAAGCTAAAAGG
UTR Short2 R	ACCAACGGCGAGTACAGTTT
actin F	GGTCGCGATTTAACCGACTACCTGAT
actin R	AGCAGATGTGGATCTCGAAGCAAGAG

Table S1: Primers for generating Northern blot probes

The above primers are used to generate radioactive Northern blot probes. ORF - Open Reading Frame of *pros* transcript; UTR Long are used to generate probes that are specific to the 15 kb *pros* 3' UTR (probe LONG); UTR Short are used to generate probe that is against region that is common to all *pros* 3' UTRs (probe ALL).

Name	Sequence (5' - 3')
Oligo d(T)	TGCATGCGGCCGCTTTTTTTTTTTTTTT
pros 15 kb F	TTCGGACGTTGTATGCACCA
pros 3 kb F	GCGGGCGTTAGGGTAGTTAAA
pros 1 kb F	CGCAGGCCAAAGCTAAAGG
pros 200 F	GCAAGCGACAAAATCGATAGACA

Table S2: Primers for Poly(A) site mapping

Oligo d(T) was used in pair with primers that is specific to *pros* 3' UTR. Four predicted poly(A) sites were tested occurring 212 base-pair (bp) (*pros 200F*), 1355 bp (*pros 1 kb F*), 3265 bp (*pros 3 kb F*) and 15,530 bp (*pros 15 kb F*) after stop codon.

Name	Sequence (5' - 3')
rp49 F	GCTAAGCTGTCGCACAAA
rp49 R	TCCGGTGGGCAGCATGTG
pros F	TATGCACGACAAGCTGTCACC
pros R	CGACCACGAAGCGGAAATTC

Table S3: Primers used for RT-qPCR for Syncrip and IgG immuno-precipitation experiments

pros and housekeeping gene *rp49* was used to assess the efficiency and specificity of Syncrip binding to *pros*.